Department of Aerospace Engineering

University of Cincinnati

THE EFFECT OF AMBIENT CONDITIONS ON CARBON MONOXIDE EMISSIONS FROM AN IDLING GAS TURBINE COMBUSTOR

A thesis submitted to the

Department of Aerospace Engineering and Applied Mechanics
College of Engineering
Division of Graduate Studies
UNIVERSITY OF CINCINNATI

in partial fulfillment of the
requirements for the degree of

Master of Science

1977

by

ANAND K. SUBRAMANIAM

B. Tech. Indian Institute of Technology Madras, 1975
(Aeronautical Engineering)

ABSTRACT

Changes in ambient temperature and humidity affect the exhaust emissions of a gas turbine engine. The results of a test program employing a JT8D-17 combustor are presented which quantize the effects of these changes on carbon monoxide emissions at simulated idle operating conditions. Analytical results generated by a kinetic model of the combustion process, and reflecting changing ambient conditions, and a comparison of these with the experimental results are also given. It is shown that for a complete range of possible ambient variations, significant changes do occur in the amount of carbon monoxide emitted by a gas turbine at idle, and that the analytical model is reasonably successful in predicting these changes.

TABLE OF CONTENTS

ACKNOWLEDGEMENTS

The author would like to express his sincere appreciation to Professor C.W. Kauffman for his patience, guidance and useful criticism during the course of this research effort.

I would like also, to place on record my gratitude to the University of Cincinnati for providing financial support and to the NASA Lewis Research Center for providing the funding for this research effort under NASA Grant NSG 3045.

Thanks are also due to Mr. H.F. Butze of the NASA Lewis Research Center for his assistance in obtaining the experimental data and to Donna Bollmer for providing secretarial support.

LIST OF FIGURES

LIST OF FIGURES (Continued)

Figure

LIST OF TABLES

NOMENCLATURE

f/a	fuel/air ratio
f/o	fuel/oxidizer ratio
H_i	mass fraction of species i
m_i	mass of species i
PR	pressure ratio
RH	relative humidity
T_o	ambient temperature
T_3	combustor inlet temperature
T_4	combustor discharge temperature
W_s	specific humidity
γ	ratio of specific heats
η_c	compressor efficiency
τ	residence time

Subscripts

b	burnt gas
d	dilution zone
o	oxidizer
p	primary zone
s	secondary zone

INTRODUCTION

Aircraft gas turbine engines utilize hydrocarbon fuels, which are allowed to burn inside the combustion chambers of the engine, resulting in heat release, which is converted to motive power by the turbine and the nozzle. The burning process also results in the predominant products of hydrocarbon-air combustion, namely, carbon dioxide and water. However, the combustion process is not ideal, and small amounts of other products are also formed. These auxiliary products may be categorized as the products of incomplete combustion, oxides of nitrogen, and products arising out of impurities in the fuel. The products of incomplete combustion include carbon monoxide, unburnt hydrocarbons and smoke; the oxides of nitrogen include nitric oxide and nitrogen dioxide, collectively called NO_x; impurities in the fuel give rise to other products such as oxides of sulfur.

Smoke and NO_x emissions are found to occur in quantity when the engines are operating under high power settings. Smoke has been identified as being produced in the fuel-rich regions of the combustor, and by proper combustor design, taking care to avoid such regions, smoke emission has been significantly reduced. Production of oxides of of nitrogen in quantity arises out of extended contact between oxygen and nitrogen in the air at high temperatures within the combustor.

Carbon monoxide and unburnt hydrocarbons are produced in quantity under low power settings of the engine. At such settings, both the mass flows of air and fuel are low, but the mass flow of air is much higher than that of the fuel, resulting in very lean primary zones. Carbon monoxide and unburnt hydrocarbons result from such zones, because the flame is relatively cold at the low fuel/air ratios encountered here, due to which, oxidation of carbon monoxide and hydrocarbons is inhibited.

These emissions, namely, oxides of nitrogen, smoke, carbon monoxide, and unburnt hydrocarbons have been called "pollutants" by the United States Environmental Protection Agency. While the actual amounts of these pollutants discharged from a single engine may be diminutive, it is important to note that these emissions occur entirely in the vicinity of air transportation centers, at the ground level, and that thousands of engines may be operated in the course of a single day. Engines operate under low power settings during idling and taxiing, and under high power settings during take off. The consequent release, into the local environment, of large amounts of these pollutants is of great concern.

Programs are in progress to assess the actual impact of such emissions from aircraft gas turbine engines, and other sources, on the earth's environment, on the climate patterns, on the inhabitants, and on vegetation. It is

beyond doubt that there are both localized and dispersed effects[2]. In addition to just vitiating the atmosphere, there is the danger of setting in motion other reactionary processes which may result in irreversible consequences. The global impact of pollution on the climate is of great concern, but is yet to be recognized. However, short-term and localized effects such as smog, effects on vegetation and adverse physiological effects on humans are well-known. The danger of depleting the earth's protective ozone layer in the stratosphere and consequently raising the levels of undesirable ultra-violet radiation at the earth's surface, cuasing physiological problems such as skin cancer, is also of great concern. This is an example of the possible long-term effects of indiscriminate pollution, and indicative of the gravity of the situation, if the pollution problem is not taken well in hand, at an early stage.

Towards this goal, namely, to limit pollution from future powerplants, the USEPA made a detailed study of the situation and issued a set of regulations. For aircraft gas turbine engines, in particular, standards were issued in 1973[1]. These standards were in the form of EPA parameters, or EPAP's, and were given as the emission index over a landing/take-off cycle. The emission index is defined as the grams of pollutant released per kilogram of fuel consumed. Engines, whose pollution levels exceeded these limits would not be certified for operation. Also, the

EPAP's related to pollution levels at standard day conditions of 1 atmosphere pressure, 289°K temperature, and zero humidity (the standard humidity has been changed to 60% relative humidity). Since actual atmospheric conditions rarely meet the standard day criteria, and since emission index measurements made for certification purposes may vary, depending on the particular ambient conditions of measurement, it is necessary to have a method for correcting non-standard emission index measurements for ambient condition variations. Towards this end a correction factor was defined, as follows:

$$\text{Correction Factor} = \frac{\text{Emission Index under Standard Conditions}}{\text{Emission Index under Nonstandard Conditions}}$$

Knowing the nonstandard conditions of measurement and thus the relevant correction factor, a priori, and the measured emission index (nonstandard), simple multiplication of the two will result in the emission index which would have occurred (for the particular engine), had the conditions of measurement been standard atmospheric day conditions.

Additionally, it is desirable to have a general equation, at least applicable to one particular type of engine, for the correction factor, incorporating ambient and other effects. This and similarity between different engine types would greatly ease the regulatory task of enforcing the EPA standards. Correction factor correlations, including ambient temperature, pressure, and humidity effects are

therefore desired.

Quite early, Lipfert[3] noted the effects of changes in inlet pressure, temperature, and humidity on the emission levels of oxides of nitrogen, produced by an engine operating under take-off power conditions. Subsequently, numerous correction factor correlations were formulated. A compilation and evaluation of these and other correction factors have been given by Rubins and Marchionna[4]. For a combustor operating at idle, Marzeski and Blazowski[5] developed additional correlations for the effects of nonstandard ambient pressure and temperature on all emissions. For production samples of a given engine, the effect of ambient temperature and pressure on all emissions over the complete thrust range has been correlated by Sarli et al.[6].

With the exception of some limited engine test results given by Nelson[7], Mosier et al.[8], and the work reported by Allen and Slusher[9], the effect of humidity on carbon monoxide emissions from idling gas turbine combustors has received little attention, although the extreme sensitivity of carbon monoxide oxidation to the presence of water vapor is well-known.

To ascertain the effects of ambient conditions, humidity in particular, on carbon monoxide emissions from idling gas turbine combustors, a two-pronged research effort was initiated, encompassing both experimental and analytical

work. Experimentally, a combustor rig was employed to simulate changing combustor inlet conditions as generated by changing ambient conditions, and carbon monoxide emission levels were measured at the combustor exit for each simulated ambient condition. The results revealed that ambient humidity and temperature can, indeed, have significant effects on carbon monoxide emission levels.

As far as the analytical effort is concerned, it is well known that equilibrium considerations lead to erroneous results, in that the predicted carbon monoxide levels can differ from measured levels by several orders of magnitude. Hence, chemical kinetic considerations may be more appropriate in describing the combustion process in a gas turbine combustor. It is also reasonable to construct a combustor model, with provisions for incorporating both local combustor conditions and ambient conditions, in order to be able to compute the carbon monoxide emission levels with respect to changes in ambient conditions. Some details relevant to carbon monoxide production in gas turbine combustors have been given by Morr et al.[10], and a less detailed model, but including limited ambient effects has been presented by Sarli et al.[6]. A review of various gas turbine combustor modelling concepts and emissions has been given by Osgerby[11], wherein sophisticated combustor models employing perfectly stirred reactors, partially stirred reactors and combinations of these and plug-flow reactors, such as in what is known as a

"Swithenbank model" are also discussed.

In attempting to define a tractable, yet accurate model of the combustor, conflicts will arise. It must be borne in mind that even sophisticated combustor models have not been totally satisfactory in predicting emission levels. Further, the increased complexity and sophistication in computation techniques, necessary when such models are employed, may, in fact, obscure the principal features of pollutant production, and also result in high computation costs.

Plug-flow reactor models, in comparison, are known for their simplicity and ease of computation. Reasonable results have been obtained using plug-flow reactors in combustor modelling[12],[13],[14]. In the interests of simplicity, ease of computation, reduced cost of computation, and retention of the principal features of pollutant production, plug-flow reactor modelling is employed in this research effort. In the analytical program, a chemical reaction kinetic scheme was applied in the combustor modelling, where initial species concentrations reflected both combustor characteristics and changing ambient conditions.

The goals of the present work are to present a simple combustor model and to apply this model to predict the effects of ambient temperature and humidity on the carbon

monoxide emission levels from an idling gas turbine combustor, to develop correction factors for these effects and to compare the calculated and measured emission levels and correction factors.

EXPERIMENTAL PROGRAM

The aims of the experimental program are to measure carbon monoxide emission levels from gas turbine combustors operating under idling conditions for various simulated ambient temperatures and humidities, and to ascertain their effects on the emission levels.

The experimental program was conducted at the NASA Lewis Research Center, employing their closed-duct test facility, which is described in detail by Fear[15]. This facility consists of a combustor rig, with provisions for supplying appropriate amounts of humidified non-vitiated air at conditions which simulate various compressor pressure ratios, at the combustor inlet.

A single JT8D-17 combustor can was installed in the duct, along with the appropriate instrumentation for measuring static pressure, total temperature and gas chemical composition as shown in Fig. 1. The can was supplied with appropriate amounts of non-vitiated air and Jet A fuel to maintain a constant overall fuel/air ratio. Demineralized water was injected well upstream of the combustor inlet, to insure complete vaporization, in order to simulate ambient humidity. The temperature, pressure, and humidity at the combustor inlet were controlled to reflect desired ambient conditions, pressure ratios, and compressor efficiency.

Humid air and fuel were allowed to undergo combustion in the JT8D-17 can under these simulated conditions, and the total temperature, static pressure, and chemical composition were measured to SAE specifications [16] at the various locations shown in Fig. 1.

Test Conditions

The idle operating conditions, both nominal and as tested, are given in Table I. In relating ambient variables to combustor inlet variables, compressor pressure ratios of 2, 3, 4 and 5 were chosen, along with a compression efficiency of 80 percent. The mass flow through the combustor consists of both air and water vapor, the combination of which may be regarded as the oxidizer. The fuel flow was controlled to maintain a constant fuel/air ratio and not a constant fuel/oxidizer ratio. The actual mass flow through the combustor was calculated on either a constant compressor discharge Mach number basis, or a constant reference velocity basis. Also, since the combustor geometry was fixed, three different values of overall fuel/air ratio were run, in order to affect local fuel/air ratios within the combustor.

The combustor inlet pressure, temperature, and humidity were controlled to reflect desired ambient conditions of 244, 289 and 322°K temperature and 0, 50 and 100 percent relative humidity, except at 244°K, at which temperature

an extremely small amount of water vapor corresponds to saturation, so only one value of relative humidity could be obtained, which was approximately 60 percent. The water content of the air supplied by the preheater was continually monitored and was quite small.

Experimental Results

Representative values of the measured carbon monoxide emissions from the JT8D-17 combustor can are given in Figs. 2, 3, 4 and 5, in terms of the carbon monoxide emission index against the average combustor discharge temperature.

Each separate figure corresponds to one simulated compressor discharge condition - a pressure ratio of 3 or 4, and either a constant compressor discharge Mach number or a constant reference velocity. On each figure, three sets of data are presented, one for each overall fuel/air ratio of 0.015, 0.011 and 0.007.

Identically-shaded symbols correspond to one particular fuel/air ratio, differently flagged symbols depict the effect of ambient temperature, and identically flagged different symbols depict the effect of humidity. The various pressure ratios, compressor discharge conditions, and appropriate symbol legend are given in the figures. The effects of ambient temperature and humidity are felt both on the combustor discharge temperature and the carbon monoxide emission index as follows:

As regards the combustor discharge temperature:

(i) For all other conditions remaining unaltered, a larger fuel/air ratio gives a higher combustor discharge temperature (compare differently shaded symbols).

(ii) For a fixed fuel/air ratio, and zero humidity, the combustor discharge temperature increases as ambient temperature is increased (compare identically shaded circular symbols).

(iii) For a fixed fuel/air ratio and ambient temperature, an increase in the relative humidity leads to a decrease in the combustor discharge temperature (compare identically shaded, identically flagged symbols).

As regards the carbon monoxide emission index:

(i) For a fixed set of ambient conditions, an increase in the fuel/air ratio leads to a decrease in the carbon monoxide emission index (compare differently shaded symbols).

(ii) For a fixed fuel/air ratio and zero humidity, an increase in the ambient temperature causes a decrease in the emission index (compare identically shaded, differently flagged circular symbols).

(iii) For a fixed fuel/air ratio and given ambient temperature, an increase in the relative humidity leads to an increase in the emission index, an effect especially noticeable at the highest ambient temperature of 322°K, where saturation corresponds to 8.12 percent by mass of water

vapor (compare identically shaded, identically flagged, symbols).

(iv) For all fuel/air ratios, the slope $\left(\frac{\partial EI_{CO}}{\partial T_4}\right)_{RH=0\%}$ is nearly identical.

(v) The slope $\left(\frac{\partial EI_{CO}}{\partial T_4}\right)_{RH=100\%}$ increases with decreasing fuel/air ratio.

(vi) At the highest fuel/air ratio, 0.015, the slopes $\left(\frac{\partial EI_{CO}}{\partial T_4}\right)_{RH=0\%}$ and $\left(\frac{\partial EI_{CO}}{\partial T_4}\right)_{RH=100\%}$ are nearly identical.

As regards the basic trends noted above, there is little difference between a constant reference velocity condition or a constant compressor discharge Mach number condition. However, a comparison of figures corresponding to pressure ratios of 3 and 4 reveal that a decrease in the pressure ratio, for both the above conditions, leads to an increase in the carbon monoxide emission index. Emissions data collected at other simulated pressure ratios reflect similar trends with regard to changing ambient conditions.

Other combustor data is also surprisingly similar. The emissions data of Blazowski et al.[5] for a T-56 combustor, employing two different fuels under idle conditions, but with different primary zone characteristics is presented in Fig. 6 in a form similar to the JT8D-17 data. During these tests, the geometry of the combustor

was modified slightly, to allow adjustment of the primary zone fuel/air ratio, while keeping the overall fuel/air ratio unaltered. The relative humidity was close to zero and the simulated compressor pressure ratio was three. Although there are differences in the actual carbon monoxide emission index produced by the JT8D-17 and the T-56 combustor under idle conditions, the slope:

$$\left(\frac{\partial EI_{CO}}{\partial T_4}\right)_{RH=0\%}$$

in both figures 5 and 6, depicting the ambient temperature effect is nearly identical, especially for the lean primary zone of the T-56. Such a similarity between different combustors, if discovered, would considerably ease the regulatory task of developing corrections for nonstandard ambient conditions.

ANALYTICAL PROGRAM

The experimental results indicate that carbon monoxide emission levels are decreased by an increasing fuel/air ratio, pressure ratio, and ambient temperature, while they are increased by an increasing ambient humidity. In order to understand this behavior it would seem reasonable to construct a combustor model. Several factors are of importance when such a model is desired, in order to be able to predict pollutant emission levels from gas turbine combustors. A typical gas turbine combustor consists of a casing to contain the air flow, within which, there is a means for mixing fuel and air, and burning the mixture under stable conditions. The actual combustion process is extremely complex, and includes recirculation of burnt products, incomplete mixing, delay in mixing and burning, quenching by the walls of the combustor, and further, these processes occur simultaneously. Detailed investigations by Mellor et al.[17],[18] of gas turbine combustors have revealed the existence of such complex processes in the confines of combustors.

A realistic computational model of the combustor would have to incorporate all these complexities, and in addition, have provisions for taking into account the effects of ambient conditions on the operating parameters, such as pressure, temperature, and chemical composition.

However, it has not been possible to include these effects and have a reasonable computation time, and hence simpler models are highly desirable.

The combustion process in a gas turbine combustor is known to generally occur in three principal zones: the primary, secondary, and dilution. These zones are shown for a typical gas turbine combustor in Fig. 7. The primary zone consists of a fuel injection region and a highly stirred region. Most of the combustion, to the extent of 90 percent, occurs in this zone. The secondary zone completes the combustion to about 99 percent and initiates dilution, which is completed in the dilution zone, to provide an acceptable turbine inlet temperature. All combustor models so far suggested invariably subdivide the combustor into these three zones, and differ basically in the manner in which the primary zone is modeled, consideration of droplet evaporation and combustion, and in the chemistry of pollutant production. A detailed discussion of these aspects is given in a review paper by Osgerby[11].

In the model presented in this research effort, it is suggested that each such zone within the combustor be treated as a plug-flow reactor. In a plug-flow reactor of the type employed in this analysis, there is homogeneous chemical reaction between perfectly mixed fuel and

oxidizer, under conditions of constant pressure and temperature. The pressure here depends on the ambient pressure and compressor pressure ratio, and the temperature is taken as the adiabatic flame temperature for each particular ambient condition and local fuel/air ratio. In actuality, adiabatic flame temperatures are not attained in the combustion zones due to the fact that chemical equilibrium is not reached in the combustor. The chemistry in such plug flow zones may be described adequately by a set of chemical reactions, or kinetics. Since the actual kinetics representing the oxidation of a hydrocarbon fuel such as Jet A are only poorly understood, a simpler fuel, methane, whose oxidation kinetics are well documented, is employed.

It is in keeping with one of the goals of this research effort, namely, simplicity, that plug-flow reactors are being used to model the combustor. Plug-flow models ignore all the complexities in the flow previously mentioned, and provide an idealization of the combustion process. However, they need not be considered as over-simplifying the matter, because even relatively sophisticated combustor models have not been totally satisfactory in accounting for pollutant emission levels. Some of these sophisticated models are presented and discussed in detail by Morr et al.[10], Osgerby[11], Sheppard[19], Pratt et al.[20], and

Boccio et al.[21]. Plug-flow models on the other hand, have been used with limited success by Seery and Bowman[12] Marteney[13], and Starkman et al.[14]. Further, complex combustor models require sophisticated computation techniques which indeed obscure the principal features of pollutant production. In the interests of simplicity and reduced computation time and costs, plug flow modelling is employed in this research effort.

As mentioned earlier, plug flow reactors allow perfectly mixed fuel and oxidizer to undergo chemical reaction in a constant pressure, constant temperature environment. The temperature in a plug flow reactor corresponds to the adiabatic flame temperature which is calculated using the NASA CEC-71 computer program[22]. The computer program requires, as input, the reactant composition, pressure, and initial temperature. The reactant composition reflects the ambient humidity, and the initial temperature reflects the ambient temperature, the pressure ratio, and the compressor efficiency. The reactant inlet temperature, (i.e., at combustor inlet) is given by:

$$T_3 = T_o \left[1 + \frac{1}{\eta_c} \left\{(PR)^{\frac{\gamma-1}{\gamma}} - 1\right\}\right] \qquad (1)$$

For an explanation of the symbols, please refer to the "Nomenclature".

The initial chemical composition of the reactants, which consist of fuel and oxidizer, are calculated as follows:

Oxidizer: (Proportions by mass)

Nitrogen	(N_2)	0.7555
Oxygen	(O_2)	0.2313
Argon	(Ar)	0.0127
Carbon Dioxide	(CO_2)	0.0005
Dry Air		1.0000

(2)

$$\text{Water Vapor } (H_2O) = \text{Dry Air} \times W_s \times RH$$
$$= 1 \times W_s \times RH = W_s \times RH \quad (3)$$

$$\text{Oxidizer total mass} = \text{Dry Air} + \text{Water Vapor}$$
$$= 1 + (W_s \times RH) \quad (4)$$

The mass fraction of each component in the oxidizer is given by:

$$\text{Nitrogen} = 0.7555 / (1 + W_s \times RH) ,$$
$$\text{Oxygen} = 0.2313 / (1 + W_s \times RH) ,$$
$$\text{Argon} = 0.0127 / (1 + W_s \times RH) ,$$
$$\text{Carbon Dioxide} = 0.0005 / (1 + W_s \times RH) , \text{ and}$$
$$\text{Water} = W_s \times RH / (1 + W_s \times RH) . \quad (5)$$

The fuel consists of methane which is given by:

$$\text{Methane } (CH_4) = \text{Dry Air} \times \text{fuel/air}$$
$$= 1 \times f/a = f/a \quad (6)$$

Also, $$\text{Methane} = \text{Wet Air} \times \text{fuel/oxidizer}$$
$$= (1 + W_s \times RH) \times (f/o) \quad (7)$$

The relative amounts by weight, of the various components comprising the reactants and their initial states can now be calculated, if the fuel/air ratio or fuel/oxidizer ratio and the ambient conditions and pressure ratio are specified. For each such specific condition, the NASA CEC-71 computer program calculates the adiabatic flame temperature and equilibrium chemical composition.

The kinetic chemical calculations in the plug flow reactors is carried out using the NASA GCKP[23] computer program. This program calculates the time history of the initial chemical species concentrations, given the initial conditions of pressure, temperature and composition by integrating rate equations. Other constraints are also possible, such as keeping pressure and temperature unaltered. The input to this program requires, in addition to the initial conditions, a chemical reaction kinetic scheme to describe the combustion process.

Depending on whether there is mixing of burnt gas and fresh air, to simulate addition of air, or not, i.e.

depending on whether the kinetic calculations are to be performed for the secondary and dilution zones, or the primary zone, respectively, the initial species concentrations are calculated in a slightly different manner. In the primary zone, the fuel and oxidizer are assumed to be perfectly mixed instantaneously and the initial mass fractions are calculated as follows.

$$\begin{aligned}
\text{Dry Air} &= N_2 + O_2 + Ar + CO_2 \\
&= 0.7555 + 0.2313 + 0.0127 + 0.0005 \\
&= 1.0000
\end{aligned}$$

$$\text{Water Vapor} = H_2O = \text{Dry Air} \times W_s \times RH = 1 \times W_s \times RH = W_s \times RH \, .$$

$$\text{Fuel} = CH_4 = \text{Dry Air} \times f/a = 1 \times f/a = f/a \, .$$

$$\text{Total mass of initial species} = (1 + W_s \times RH + f/a) \tag{8}$$

The mass fractions of each species:

$$\begin{aligned}
N_2 &= 0.7555 \,/(1 + W_s \times RH + f/a) \, , \\
O_2 &= 0.2313 \,/(1 + W_s \times RH + f/a) \, , \\
Ar &= 0.0127 \,/(1 + W_s \times RH + f/a) \, , \\
CO_2 &= 0.0005 \,/(1 + W_s \times RH + f/a) \, , \\
H_2O &= W_s \times RH/(1 + W_s \times RH + f/a) \, , \text{ and} \\
CH_4 &= (f/a) \,/(1 + W_s \times RH + f/a) \, .
\end{aligned} \tag{9}$$

A FORTRAN program given in Appendix 1 performs the above calculations and produces results on punched cards, ready for use in the chemical kinetic calculations computer program.

When there is mixing of burnt gas and fresh air, as is the case during entry to the secondary and dilution zones, where the burnt gases from the previous zone are mixed with appropriate amounts of air, to lower the fuel/air ratio, the initial species concentrations (mass fractions) for use in the kinetic calculations program, are calculated with the aid of the FORTRAN program in Appendix 2 as follows.

Consider the case where it is required to calculate the initial species concentration during entry to the secondary zone. Burnt gases from the primary zone are instantaneously mixed perfectly with fresh secondary air, and then allowed to burn in the secondary zone. The fuel/oxidizer ratios in the primary and secondary are $(f/o)_p$ and $(f/o)_s$ respectively. This situation can be considered as starting out with a certain amount of fuel, f, and the appropriate amount of oxidizer, namely $f/(f/o)_s$, which will result in a fuel/oxidizer ratio of $(f/o)_s$ in the secondary, feeding part of this oxidizer through the primary, namely $f/(f/o)_p$, and feeding in the rest of the oxidizer, namely $f\cdot\{1/(f/o)_s - 1/(f/o)_p\}$ as secondary air, which is mixed with the effluents from the primary zone combustion, to simulate entry into the secondary zone.

The mass fractions of the burnt gas mixture are obtained from the results of plug flow calculations applied in the primary zone. The mass fractions of the secondary air are the same as those for fresh air, depending on ambient conditions. The mass of the burnt gas consists of the mass of primary air and injected fuel, and the mass of the secondary air is the rest of the oxidizer mass as mentioned above. The masses of individual species in the burnt gas and secondary air are then given by multiplying the total mass of either the burnt gas or secondary air, with their respective mass fractions. Instantaneous mixing of these two result in a different composition, calculated as given below.

Burnt gas individual species mass:

$$m_{b_i} = H_{b_i} \times (f + f/(f/o)_p) \tag{10}$$

Secondary oxidizer individual species mass:

$$m_{b_i} = H_{o_i} \times (f/(f/o)_s - f/(f/o)_p) \tag{11}$$

After instantaneous mixing, individual species mass:

$$m_i = m_{b_i} + m_{o_i} \tag{12}$$

After mixing total mass:

$$M = \sum_i m_i = \sum_i m_{b_i} + m_{o_i} \tag{13}$$

The mass fractions at secondary zone entry:

$$H_i = \frac{m_i}{M} = \frac{m_{b_i} + m_{o_i}}{\sum_i m_{b_i} + m_{o_i}}$$

i.e.

$$H_i = \frac{H_{b_i}[1 + 1/(f/o)_p] + H_{o_i}[1/(f/o)_s - 1/(f/o)_p]}{\sum_i H_{b_i}[1 + 1/(f/o)_p] + H_{o_i}[1/(f/o)_s - 1/(f/o)_p]} \quad (14)$$

These H_i are the mass fractions at the entry to the secondary zone. The mass fractions at the entry to the dilution zone are calculated in the same manner, by considering the primary and secondary zones to be one unit, replacing the primary zone in the calculations, and considering the dilution zone as the secondary zone.

To describe the combustion process, a kinetic chemical reaction scheme is also required. A list of reactions employed for this purpose is given in Table II. These reactions describe the quick breakdown of the methane fuel into radicals and carbon monoxide, and their subsequent oxidation to final products of water and carbon dioxide, and also other radical recombinations. In addition, the kinetics of the formation of oxides of nitrogen are also included. Table II also gives the forward rate constant associated with each reaction. Table IIa gives the different reaction schemes actually employed in the analytical program.

A 30 reaction scheme (number 1) was first employed in a pilot analytical effort to ascertain whether humidity had any effect on carbon monoxide production. This scheme is given and discussed in detail in a review paper by Osgerby[11] and includes reactions to describe burn up of methane, production and consumption of carbon monoxide, and production of both nitric oxide and nitrogen dioxide.

A 20 reaction scheme (number 2), which is essentially the same as the one used by Ay and Sichel[24], is also given in the same tables. The differences between schemes 1 and 2 are that the latter does not include the kinetics of nitrogen dioxide production, some auxilliary reactions for nitric oxide production and a carbon monoxide production reaction. Table IIa gives the details. In carbon monoxide kinetics, the reaction $CO + OH = CO_2 + H$ has been shown to dominate the oxidation process by Westenberg[25], and nitric oxide kinetics have been adequately described by the mechanism proposed by Zeldovich[26].

The reaction scheme 3 consists of the same 20 reactions, but with a modified forward rate constant for the $CO + OH = CO_2 + H$ reaction. This rate constant is similar to the one developed by Kollrack[27] and was chosen for its large temperature dependence.

A. Analytical Models:

A typical gas turbine combustor is shown in Fig. 7, wherein the combustor is subdivided into the three familiar zones, the primary, secondary and dilution. Combustion occurs in each of these three zones accompanied by complex flow processes. In the analytical model, these processes are ignored and simple plug-flow reactors are employed to simulate combustion in the three zones, one for each zone as shown in Fig. 8.

In the primary zone, fuel and oxidizer, taken in appropriate amounts to simulate a particular fuel/air ratio in the primary zone, are instantaneously mixed and allowed to undergo chemical reaction at a pressure of 4 atmospheres (compressor pressure ratio is four) and at a temperature corresponding to the adiabatic flame temperature which reflects both ambient conditions and fuel/air ratio. The reaction process is allowed to proceed for 5 msec., which is taken as representative of a primary zone residence time. The initial species composition is calculated using the FORTRAN program given in Appendix 1, and the chemical composition of the primary zone effluents, using the NASA GCKP computer program, developed by Bittker and Scullin[23].

These effluents are then perfectly mixed, instantaneously, with precalculated amounts of fresh air in the manner explained in the previous section, using the

FORTRAN program given in Appendix 2 to simulate entry into the secondary zone. The fuel/air ratio in the secondary zone is lower than that in the primary zone and hence the temperature is also lower. Using the same NASA GCKP program, the chemical composition of the mixture after a secondary zone residence time of 5 msec. is calculated. The conditions in the secondary zone are once again modeled as a plug-flow reactor. The secondary zone effluents are once again mixed with an additional amount of fresh air to simulate entry into the dilution zone in the same manner as above, and the mixture allowed to undergo chemical reaction in the plug-flow reactor modeling the dilution zone, and the chemical composition calculated after a dilution zone residence time of 5 msec. This composition is taken to be that at the combustor exit. Carbon monoxide mole fractions, reflecting various ambient conditions and fuel/air ratios, in particular, are noted.

This type of combustor modelling applies for schemes which assume the primary zone to be fuel-rich. However, as stoichiometric primary zone fuel/air ratios are approached, a slightly modified combustor model is necessary. The details of the modifications are given in what follows.

It is suggested that at near and below stoichiometric primary zone fuel/air ratios, homogeneous single phase combustion may not occur, but that individual fuel droplet burning may dominate the combustion. Actual burning occurs around individual droplets under stoichiometric conditions and the products of this combustion are immediately quenched by the surrounding air to lower fuel/air ratios, in the primary zone itself. This has the effect of "freezing" the highest carbon monoxide levels which occur during droplet combustion. Indeed, experimental evidence given by Sullivan[28], indicates that this type of primary zone quenching does occur. Sullivan found that the exact placement of air holes in the secondary zone had very little effect on the carbon monoxide emission levels, suggesting that these levels are quenched by surrounding primary air itself and any additional air would make very little difference except in lowering the mass fractions because an additional mass of air is introduced.

To model this type of behavior, the primary zone is considered as comprising two combustion phases. The first phase is the individual droplet burning and the second phase is the immediate dilution by surrounding primary air. As shown in Fig. 9, each such zone is modeled as a plug flow reactor. The first reactor has a temperature and initial species concentration reflecting ambient conditions

and for a stoichiometric or slightly rich fuel/air ratio. Chemical reaction occurs in this zone for a very short period of time, 0.1 msec., which is of the same order as the time taken by a flame front to travel through the near-stoichiometric combustion zone surrounding individual droplets. The products of this combustion zone are now mixed with fresh air to bring the fuel/air ratio, and hence the temperature down, simulating the process of immediate dilution of droplet burning products, and the mixture allowed to undergo chemical reaction in the second primary plug flow reactor for 5 msec., representative of a primary zone residence time.

Subsequently, these products are allowed to pass through the secondary and dilution zones again modeled as plug flow reactors, in the same manner as for the previous model. The chemical composition, carbon monoxide mole fraction in particular, is noted at the end of the dilution zone.

In the analytical model presented here, various fuel/air ratio combinations were considered, and the various parameters relevant to one of these values, namely an $f/a)_d$ of 0.011, are given in Table III. Experimentally, the combustor was operated under conditions corresponding to the primary, secondary, and dilution zone fuel/air ratios given in the table. For an overall or dilution zone fuel/air ratio of

0.011, the secondary and primary zone fuel/air ratios lie between 0.034 and 0.019, and 0.071 and 0.048, respectively. A comparison of the analytical and typical values of fuel/air ratio reveals a sufficient range in the variation of the typical values to include analytical values. However, differences in the residence times in each zone are apparent. In the primary zone, the actual residence is between 1.90 and 1.60 msec, whereas the analytical model takes this as 5.0 msec. This may be justifiable because chemical equilibrium is quickly attained in the primary zone, due to large reaction rates, and there is practically no difference between the carbon monoxide mole fraction after 1.0 msec. or after 5.0 msec. residence time in the primary zone, as per calculations. This situation is illustrated in Fig. 10, which is a plot of the carbon monoxide mole fraction obtained from equilibrium and kinetic calculation for various fuel/air ratios. In the entire range of values investigated, there is very little difference between the two mole fractions. However, deviations become apparent as either very lean or very rich mixtures are considered.

The secondary zone residence time can be seen from Table III, to be of the same order in both the typical combustor and the analytical model. It will be shown later in the section on analytical results, that the secondary

zone parameters play a dominant role in determining the carbon monoxide emission levels and hence the closeness in both fuel/air ratio and residence time in this zone is, indeed, necessary.

In the dilution zone, the residence time taken in the analytical model is about twice the typical value. The temperatures in the dilution zone are relatively low, with correspondingly lower reaction rates, leading to "frozen" chemistry. There is thus little change in the carbon monoxide mole fraction between 2.5 msec. and 5.0 msec. dilution zone residence time and hence the choice of the larger residence time may be justifiable.

Further, in the analytical model, methane was used as the fuel instead of JP4, which was used in the experimental program. It has already been pointed out that the primary zone carbon monoxide levels are close to equilibrium levels, as apparent from Fig. 10. It may be seen from Table IV that the equilibrium carbon monoxide mole fractions, for the same conditions, employing methane and JP4 as fuel, are of the same order, but JP4 results in a slightly higher (about one-and-a-half times) mole fraction. However, the adiabatic flame temperatures for methane are slightly lower than those for JP4, for the same conditions, resulting in slower carbon monoxide burnup when methane kinetics are employed. It is possible that these two effects may compensate for each other, at least to a limited

extent, resulting in more realistic carbon monoxide levels. It is recognized that using methane instead of JP4 is, indeed, an approximation, but because the kinetics of JP4 oxidation are only poorly understood, use of methane as the fuel may also be justifiable.

As regards the chemical kinetics employed in the analytical effort, three schemes have already been presented. The scheme number 1 has been found to be unsatisfactory in predicting carbon monoxide levels, in that the calculated mole fractions were two orders of magnitude smaller than measured values in some cases. Further, scheme number 1 also contained reactions describing the production of nitrogen dioxide, which was found to be several orders of magnitude smaller than nitric oxide, as a result of calculations. Reactions involving nitrogen dioxide were therefore considered unimportant and reaction scheme number 2, consisting of 20 reactions given by Ay and Sichel[24], which did not contain such reactions was then used. However, its use was limited to the primary zone alone, since it too underpredicted carbon monoxide mole fraction at the end of the dilution zone by two orders of magnitude. Further, the dilution zone carbon monoxide levels did not exhibit increasing trends with humidity, when this scheme was used. This led to a search for a rate constant for the carbon monoxide oxidation reaction

$CO + OH = CO_2 + H$, which is highly temperature dependent, because ambient humidity causes a decrease in the flame temperature and it is required to reduce burn-up of carbon monoxide sufficiently, as humidity is increased, in order to predict measured trends. The search resulted in the use of a rate constant developed by Kollrack[27]. This rate constant had the seventh power of the absolute temperature in the pre-exponent factor, indicating high temperature sensitivity. However, when this rate constant was used in the analysis, the carbon monoxide emission levels calculated were once again two orders of magnitude smaller than the measured levels. It was then suggested that this rate constant be reduced by a factor of ten, and when this value was used, reasonable results were obtained. Figure 11 illustrates this situation adequately. For a variety of conditions, the carbon monoxide emission level is plotted against the combustor exit temperature (dilution zone flame temperature). Comparison of measured carbon monoxide ppm levels and calculated values reveals not only good agreement in the order of magnitude, but also in the trends as regards the effects of ambient humidity and temperature.

Further, Table V gives the values of the largest and the smallest reported rate constants for the carbon monoxide oxidation reaction for various absolute temperatures.

These rate constants are taken from the work of Sorenson et al.[29]. In the secondary zone, the temperature is of the order of 1500°K, at which the used rate constant "USED K" is slightly smaller than the smallest reported value, "SMALL K". However in the dilution zone, the temperature is very low, of the order of 800°K, at which the used rate constant is slightly larger than the smallest value but smaller than the largest value, "LARGE K". The used rate constant is, indeed, relatively small, but because of good results as in Fig. 11, its use may also be justifiable.

B. Analytical Results:

The experimental results, already being ascertained, in that the principal effects of ambient temperature and humidity on carbon monoxide emission levels at the combustor exit are as follows:

(1) ambient temperature increases result in decreases in carbon monoxide level, for zero humidity and for a particular overall fuel/air ratio and compressor discharge condition, and

(2) ambient humidity increases cause increases in carbon monoxide emission levels, for a particular ambient temperature, overall fuel/air ratio, and compressor discharge conditions.

It has been possible to predict the above trends employing the analytical model described in the previous section, to a reasonable extent. The calculated results are presented here for a compressor pressure ratio of four.

Results of the adiabatic flame temperature calculations using the NASA CEC71 [22] computer program for various equivalence ratios from 0.2 to 1.3, for ambient temperatures of 244, 289 and 322°K and for relative humidities of 0, 50 and 100 percent are presented in Fig. 12. The well-known effects of ambient temperature and humidity on the adiabatic flame temperature are apparent. Ambient temperature increases produce increases in the flame temperature, for a particular equivalence ratio and zero humidity. Ambient humidity increases cause decreases in the flame temperature at any particular equivalence ratio and ambient temperature. For an ambient temperature of 244°K, Fig. 12 gives only one curve; this is because at this ambient temperature, a very small amount of water vapor corresponds to saturation and there is therefore, practically no effect on the flame temperature.

The effect of humidity on fuel/air ratios corresponding to particular equivalence ratios for various ambient humidities is given in Fig. 13. Near the stoichiometric

equivalence ratio this effect is not seen, but as one deviates from stoichiometric values, the effect is quite pronounced in that below stoichiometric values, the fuel/air ratio for humid mixtures is less than that for dry mixtures and above stoichiometric values, the reverse is true. Figure 13 contains the fuel/air values plotted against equivalence ratio for ambient temperatures of 244, 289 and 322°K and for relative humidities of 0, 50 and 100 percent for the same reason as mentioned above, there is only one curve for an ambient temperature of 244°K. The curves in Fig. 13 are useful when it is desired to determine flame temperatures for a particular fuel/air ratio, instead of for a particular equivalence ratio. Since flame temperatures in Fig. 12 are plotted against equivalence ratio, Fig. 13 can be used to determine the equivalence ratio values corresponding to a particular fuel/air ratio and various desired ambient conditions of temperature and humidity. Using these equivalence ratio values and corresponding curves in Fig. 12, the flame temperatures may be determined for the various conditions considered. The combustor is modeled as three plug-flow zones, primary, secondary and dilution, and results from calculations for each zone and relevant discussion follow.

The primary zone results are given in Fig. 14, which is a plot of the carbon monoxide correction factor CF_{CO},

against the ambient temperature, for relative humidities of 0, 50 and 100 percent, and for primary zone fuel/air ratios of 0.08, 0.07, and 0.06, the last of which is nearly stoichiometric. The correction factor has been defined as:

$$CF_{CO} = \frac{\text{Carbon monoxide mole fraction at standard conditions}}{\text{Carbon monoxide mole fraction at nonstandard conditions}}$$

with standard conditions taken as 289°K temperature and zero humidity. The mole fractions are taken after allowing fuel and oxidizer to undergo chemical reaction in the primary zone plug flow reactor for a residence time of 5 msec.

The three sets of curves in Fig. 14, one for each primary zone fuel/air ratio, are similar in nature, except for differences in the slopes. For zero humidity, in all three sets of curves, the slope of the CF_{CO} curve is negative, indicating that the carbon monoxide levels increase with increasing ambient temperature at zero humidity. At the two other relative humidities, 50 and 100%, the CF_{CO} curves have positive slopes, indicating that at these humidities, an increase in ambient temperature leads to a decrease in the carbon monoxide level. At any particular temperature, increasing humidity leads to an increase in CF_{CO}, indicating that the carbon monoxide level decreases as humidity is increased at a particular ambient temperature.

Further, products of the primary zone plug-flow reactor are almost in equilibrium, as has been mentioned earlier, with reference to Fig. 10, and thus both equilibrium and kinetic results indicate carbon monoxide trends which are to increase with ambient temperature and to decrease with ambient humidity. These trends are precisely the inverse of those measured at the combustor exit, but have been experimentally verified by Müller-Dethlefs and Schlader[30], who made measurements in rich burner flames which correspond to primary zones. These results may be explained by considering the effect of flame temperature on dissociation. It is therefore, logical to assume, in view of these results, that the subsequent secondary and dilution zones are instrumental in reversing these trends. Further, it is evident from a perusal of Fig. 14, that there are larger deviations near stoichiometric fuel/air ratios, making it increasingly difficult for the secondary and dilution zones to reverse the trends. This explains why the rich primary zone model (Fig. 8) shows signs of failure for near-stoichiometric primary zones.

The temperatures in the dilution zone are lower, hence chemical composition is somewhat "frozen"; so this zone may not have a great effect in reversing the trends. The only zone left is the secondary zone, where the temperatures

are not as low. Indeed, it turns out that the secondary zone can have a dramatic effect on the carbon monoxide levels. This is illustrated in Fig. 15, which is a plot of the carbon monoxide emission level in mole fractions at the combustor exit, against the exit temperature calculated for various secondary fuel/air ratio combinations and for various ambient conditions as shown in the figure, employing the analytical model for rich primary zones (Fig. 8). The primary zone and dilution zone fuel/air ratios are fixed, 0.07 and 0.015 respectively, but the intermediate secondary zone fuel/air ratio is varied as follows: 0.035, 0.03, 0.0275 and 0.025. However, when secondary fuel/air ratios beyond the range between 0.035 and 0.025, namely 0.04 and 0.02 for instance, are considered, the results fail to predict the trends mentioned above. The results are plotted in groups of symbols as explained in the figure, each group corresponding to one analytical scheme comprising the three combustion zones with residence times of 5 msec in each zone. Changing the secondary zone fuel/air ratio from 0.035 to 0.025 results in an order of magnitude change in the carbon monoxide mole fraction. It is thus confirmed that the secondary zone is the controlling factor as regards the carbon monoxide emission level.

While the effect of the secondary zone is evident, it is also noticed that the carbon monoxide trends with respect to ambient temperature and humidity have also been reversed. The results on Fig. 15 indicate that for each of these fuel/air ratio combinations, the analytical model is capable of predicting the observed carbon monoxide emission trends, in that for a particular analytical scheme, the carbon monoxide decreases with increasing ambient temperature (compare identically shaded circular symbols) and increases with increasing humidity at a particular ambient temperature (compare identically shaded and flagged symbols). Further, it may be noted that the largest levels of carbon monoxide are produced for smaller values of secondary fuel/air ratio, which occurs because the high CO levels in the primary zone are "frozen" by these secondary zones, where the lower temperature "quenches" the CO oxidation reaction.

Employing the same analytical model for rich primary zones (Fig. 8), additional calculations over a wide range of conditions yielded the same kind of results. Figures 16, 17 and 18 are plots of carbon monoxide mole fraction against the combustor exit temperature, which is the dilution zone adiabatic flame temperature. Three groups of results are presented in each figure, one for each fuel/air ratio combination. All three figures start out with rich primary

zones, considerably different from stoichiometric values, and subsequently undergo secondary and dilution zone combustion as follows:

$f/a)_p$	$f/a)_s$	$f/a)_d$
0.070	0.030	0.020
0.070	0.0275	0.015
0.070	0.015	0.010
0.080	0.035	0.020
0.080	0.030	0.015
0.080	0.025	0.010
0.090	0.035	0.020
0.090	0.030	0.015
0.090	0.025	0.010

The residence times in each zone was taken as 5 msec. and calculations were performed for ambient conditions of 244, 289 and 322°K temperature and 0, 50 and 100% relative humidity. In each individual case, other secondary fuel/air ratio combinations were also tried, but the analytical model gave reasonable results only for a limited range of secondary fuel/air ratio. Only such values of secondary fuel/air ratio and accompanying primary and dilution fuel/air ratio combinations are presented here. Further, these values correspond closely with

with typical combustor values, where the combustor fuel/air ratio ranged from 0.015 to 0.007.

On each figure, the effects of ambient conditions are apparent in that the trends obtained from calculations agree with experimentally observed trends as regards carbon monoxide emission levels. However, there are differences in the degree of these effects, depending on the particular choice of fuel/air ratios in the three plug flow zones. Generally, richer primary zones may be associated with richer secondary and dilution zones; doing so, and comparing results from the three figures 16, 17 and 18 for the following combinations:

$f/a)_p$	$f/a)_s$	$f/a)_d$
0.070	0.025	0.010
0.080	0.030	0.015
0.090	0.035	0.020

It may be seen that rich primary zones coupled with richer secondary and dilution zones result in lower carbon monoxide emissions in general. Also, the slopes $(\frac{\partial x_{CO}}{\partial T_4})_{RH=0.0}$ and $(\frac{\partial x_{CO}}{\partial T_4})_{RH=1.0}$ are seen to depend on the fuel/air ratio combination. For the same primary zone fuel/air ratio, and for higher values of secondary and dilution zone fuel/air ratio, both these slopes can be seen to decrease.

It was previously mentioned, in the section on the analytical models, that the model employed was only successful as applied to sequences starting out with rich primary zones. Lean primary zones may be handled in a similar manner, but with the modification that individual droplets of fuel first burn in the primary and are immediately diluted down to lean fuel/air ratios. This scheme, for lean primary zones is given in Fig. 9 and has been discussed already.

Employing this scheme then, results for two sequences starting with a primary zone with a fuel/air ratio of 0.06, which is close to the stoichiometric value, and subsequent dilution to a fuel/air ratio of 0.03 in the primary zone itself and then completing the combustion process through secondary and dilution zones with fuel/air ratios of 0.02, 0.015 and 0.010, 0.007 respectively, are shown in Fig. 19. That this model is capable of predicting the same CO trends with regard to ambient temperature and humidity changes, is evident in this figure.

Combined results for both the analytical models are given in Fig. 20, which has the carbon monoxide mole fraction plotted against dilution zone temperature, for the following sequences:

$(f/a)_{p_1}$	$(f/a)_{p_2}$	$(f/a)_s$	$(f/a)_d$
0.090	--	0.035	0.015
0.080	--	0.030	0.010
0.060	0.030	0.015	0.007

The points in the figure are in groups, one for each dilution sequence and the effects of ambient temperature and humidity can be seen to be similar for each sequence and agree with measurements. Care has been taken to couple richer primary zones with richer subsequent zones and vice versa. Once again, richer zones produce less carbon monoxide levels. These combinations fit in well with experimentally determined values of fuel/air ratio.

The analytical models have been applied over a wide range of operating conditions and have been reasonably successful in predicting carbon monoxide emission levels both as far as order of magnitude and trends with ambient conditions are concerned. In a manner similar to the experimental results, these analytical results may be summarized as follows:

As regards the carbon monoxide (mole fraction) emission level:

(i) For typical combustor conditions represented in the analytical model, the calculated carbon monoxide mole fraction (converted to ppm) and the measured values are

roughly the same because the rate constant for the carbon monoxide oxidation reaction was modified to produce these results.

(ii) For a fixed set of ambient conditions, increasing the secondary zone fuel/air ratio (and hence the dilution zone fuel/air ratio) results in a decrease in CO level.

(iii) For a fixed fuel/air ratio sequence, and zero humidity, increasing the ambient temperature causes the CO mole fraction at combustor exit to decrease.

(iv) For a fixed fuel/air ratio sequence and ambient temperature, an increase in the humidity leads to an increase in the CO emission level.

(v) The slope $\left(\frac{\partial X_{CO}}{\partial T_4}\right)_{RH=0.0}$ increases with decreasing dilution zone fuel/air ratio for any $(f/a)_p$ and $(f/a)_s$.

(vi) The slope $\left(\frac{\partial X_{CO}}{\partial T_4}\right)_{RH=1.0}$ generally increases with decreasing dilution zone fuel/air ratio, for any $(f/a)_p$ and $(f/a)_s$.

ANALYTICAL AND EXPERIMENTAL COMPARISONS

From the results of the experimental and analytical program, it may be seen that, indeed, plug-flow reactor modelling of the gas turbine combustor can be reasonably successful in predicting both carbon monoxide emission levels - with the aid of a reduced rate constant for the carbon monoxide oxidation reaction - and the effects of ambient temperature and humidity on carbon monoxide emission, with the aid of the large temperature dependence in the same rate constant.

Figure 11 presents the experimentally measured and calculated carbon monoxide emission levels (ppm) for similar combustor discharge conditions. It can be seen that the amounts of carbon monoxide calculated and measured are roughly the same, over a fairly wide range of conditions.

Figures 21, 22 and 23 present measured and calculated carbon monoxide emission levels in terms of the correction factor against ambient temperature for relative humidities of 0, 50 and 100 percent, and for various overall fuel/air ratios, which correspond to the dilution zone fuel/air ratio in the calculations. It must be kept in mind, however, that in the analytical model, each dilution zone fuel/air ratio is associated with secondary and primary zone fuel/air ratios also. These values are given in the figures.

In all these figures, the similarity in the $C_{F_{CO}}$ curves is striking. At zero humidity, these curves have a positive slope, in all three figures, indicating that the carbon monoxide levels decrease with increasing ambient temperature. The slopes of these curves for both analytical and experimental results are about the same.

However, at relative humidities other than zero, (for 50 and 100 percent), the curves obtained from the analytical program do not indicate as large an increase in carbon monoxide production as produced during the experimental measurements. The analytical model somewhat underpredicts the effect of humidity on carbon monoxide, but is, at least, successful in predicting similar trends.

Results from other experimental programs, such as those presented by Blazowski et al.[5] include carbon monoxide correction factors for ambient temperature for two different fuels JP_4 and JP_8 and for two design variations of a T-56 combustor, employing a stoichiometric and a lean primary zone. These results are plotted in Figure 24 as the correction factor against ambient temperature. "Least squares" curve fits to these data, employing linear interpolation resulted in equations for these correction factors, given in Table VI. The curve fitting was done using the BMD programs package[32]. The equations give the correction factor in terms of the pressure ratio

and ambient temperature. The effect of humidity was not investigated here, but some confidence can be gained by comparing the slopes of the zero humidity correction factor curves in Figures 21, 22 and 23 with the curves in Figure 24. The slopes and the shapes of the curves are surprisingly similar.

CONCLUSIONS

From the foregoing discussion of the experimental and analytical results, the following conclusions may be made:

1. The analytical models presented can, with limited success, predict carbon monoxide emission levels from idling gas turbine combustors. Predicted and measured levels are roughly the same. This agreement was forced by modifying the rate constant for the carbon monoxide oxidation reaction.

2. As regards prediction of the effects of ambient temperature and humidity on carbon monoxide emissions, the analytical model is able to predict the measured trends, but is unable to exactly match the slopes of these trends, in the sense, the model underpredicts the effect of humidity on carbon monoxide emissions. The effects of temperature, however, are in reasonable agreement.

3. For zero humidity, the correction factors for both the JT8D-17 and the T-56 combustor are similar; so it may be possible to have a general equation for correction factors for ambient temperature for both engines. It is one of the goals of this research effort to examine such a possibility, to help ease the regulatory task of developing corrections for nonstandard inlet conditions.

4. With simple plug-flow combustor modelling these results have been possible - one of the goals of this research effort was simplicity, which has been retained in the modelling.

5. The results indicate that carbon monoxide production in quantity is due to quenching of the primary zone products by lean secondary zones, resulting in "super-equilibrium" carbon monoxide emission levels. Gentle dilution of the primary zone will help burn-up of the carbon monoxide to a larger extent and thus result in lowered emissions. This is in agreement with results of Palmer and Seery[31].

REFERENCES

1. U.S. Environmental Protection Agency, "Control of Air Pollution from Aircraft and Aircraft Engines, Emission Standards and Test Procedures," Federal Register, 38, 136, 1973.
2. Anonymous, "Environmental Impact of Stratospheric Flight," National Academy of Sciences, Washington, D.C., 1975.
3. Lipfert, F.W., "Correlation of Gas Turbine Emissions Data," ASME Gas Turbine and Fluids Engineering Conference, San Francisco, California, March 1972.
4. Rubins, P.M. and Marchionna, N.R., "Evaluation of NO_x Prediction-Correlation Equations for Small Gas Turbines," AIAA/SAE 12th Propulsion Conference, Palo Alto, California, July 1976.
5. Marzeski, J.W. and Blazowski, W.S., "Ambient Temperature and Pressure Correction Factors for Aircraft Idle Pollutant Emissions," ASME 21st Annual International Gas Turbine Conference, New Orleans, Louisiana, March 1976.
6. Sarli, V.J., Eiler, D.C. and Marshall, R.L., "Effects of Operating Variables on Gaseous Emissions," APCA Specialty Conference on Air Pollution Measurement Accuracy as it Relates to Regulation Compliance, New Orleans, Louisiana, October 1975.

7. Nelson, A.W., "Exhaust Emission Characteristics of Aircraft Gas Turbine Engines," ASME Gas Turbine and Fluids Engineering Conference, San Francisco, California, March 1972.

8. Mosier, S.A. and Roberts, R., "Low Power Turbopropulsion Combustor Exhaust Emissions," Technical Report AFAPL-TR-73-36, July 1973.

9. Allen, L. and Slusher, G.R., "Ambient Temperature and Humidity Correction Factors for Exhaust Emissions from Two Classes of Aircraft Turbine Engines," FAA-RD-76-149, October 1976.

10. Morr, A.R., Heywood, J.B., and Fitch, A.H., "Measurements and Predictions of Carbon Monoxide Emissions from an Industrial Gas Turbine," Combustion Science and Technology, 11, 97, 1975.

11. Osgerby, I.T., "Literature Review of Turbine Combustor Modeling and Emissions," AIAA Journal, 12, 743, 1974.

12. Seery, D.J., and Bowman, C.T., "An Experimental and Analytical Study of Methane Oxidation Behind Shock Waves," Combustion and Flame, 14, 1, 1969.

13. Marteney, P.J., "Formation of Nitrogen Oxide in Hydro-Carbon Air Combustion," Combustion Science and Technology, 1, 461, 1970.

14. Starkman, E.S., Mizutani, Y., Sawyer, R.F., and Teixeira, D.T., "The Role of Chemistry in Gas Turbine Emissions," Journal of Engineering Power, Trans. of ASME, 92, Series A, 310, 1970.

15. Fear, J.S., "Performance of a Small Annular Turbojet Combustor Designed for Low Cost," NASA TMX 2476, 1972.

16. Anonymous, "Procedure for Continuous Sampling and Measurements of Gaseous Emissions from Aircraft Gas Turbine Engines," SAE ARP 1256, 1971.

17. Mellor, A.M., Anderson, R.D., Altenkirch, R.A., and Tuttle, J.H., "Emissions From and Within an Allison J-33 Combustor," Combustion Science and Technology, 6, 169, 1972.

18. Hammond, D.C., Jr., and Mellor, A.M., "Analytical Predictions of Emissions From and Within an Allison J-33 Combustor," Combustion Science and Technology, 6, 279, 1973.

19. Sheppard, C.G.W., "A Simple Model for Carbon Monoxide Oxidation in Gas Turbine Combustors," Combustion Science and Technology, 11, 49, 1975.

20. Pratt, D.T., Bowman, B.R., Robertus, R.J., and Crowe, C.T., "Comparison of Four Simple Models of Steady Flow Combustion of Pyrolyzed Methane and Air," Combustion Science and Technology, 6, 187, 1972.

21. Boccio, J.L., Weilerstein, G., and Edelman, R.B., "A Mathematical Model for Jet Engine Combustor Pollutant Emissions," NASA CR 121208, 1973.

22. Gordon, S. and McBride, B.J., "Computer Program for Calculation of Complex Chemical Equilibrium Compositions, Rocket Performance, Incident and Reflected Shocks and Chapman-Jouget Detonations," NASA SP 273, 1971.

23. Bittker, D.A. and Scullin, V.D., "General Chemical Kinetics Computer Program for Static and Flow Reactions With Application to Combustion and Shock-tube Kinetics," NASA TN D-6586, 1972.

24. Ay, J.H. and Sichel, M., "Theoretical Analysis of NO Formation Near the Primary Reaction Zone in Methane Combustion," Combustion and Flame, 26, 1, 1976.

25. Westenberg, A.A., "Kinetics of NO and CO in Lean, Premixed Hydrocarbon Air Flames," Combustion Science and Technology, 4, 59, 1971.

26. Zeldovich, Ya.B., "Oxidation of Nitrogen in Combustion," Journal of Technical Physics (USSR), 14, 3, 1944.

27. Kollrack, R., "Model Calculations of the Combustion Product Distributions in the Primary Zone of a Gas Turbine Combustor," ASME Winter Annual Meeting, New York, N.Y., 1976.

28. Sullivan, D., General Electric Company, Schenectady, New York, Personal Communication, 1977.

29. Sorenson, S.C., Myers, P.S. and Uyehara, O.A., "Ethane Kinetics in Spark-Ignition Exhaust Gases," 13th Symposium on Combustion, Salt Lake City, Utah, 1970.

30. Müller-Dethlefs, K., and Schlader, A.F., "The Effect of Steam on Flame Temperature, Burning Velocity and Carbon Formation in Hydrocarbon Flames," Combustion and Flame, 27, 205, 1976.

31. Palmer, H.B. and Seery, D.J., "Chemistry of Pollutant Formation in Flames," Annual Review of Physical Chemistry, 24, 235, 1973.

32. Anonymous, "Biomedical Computer Programs," University of California Press, 1975.

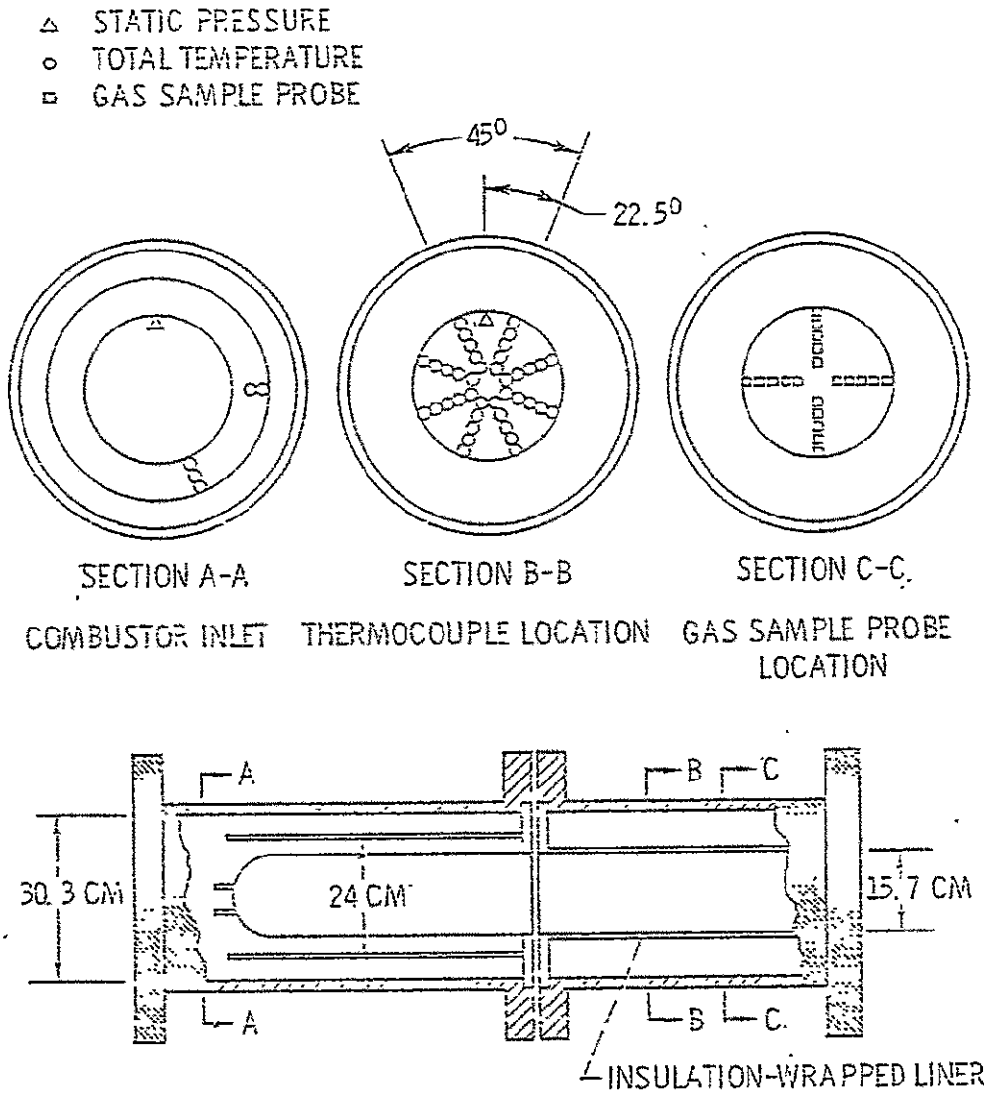

FIGURE 1. COMBUSTOR ASSEMBLY AND INSTRUMENTATION SECTIONS.

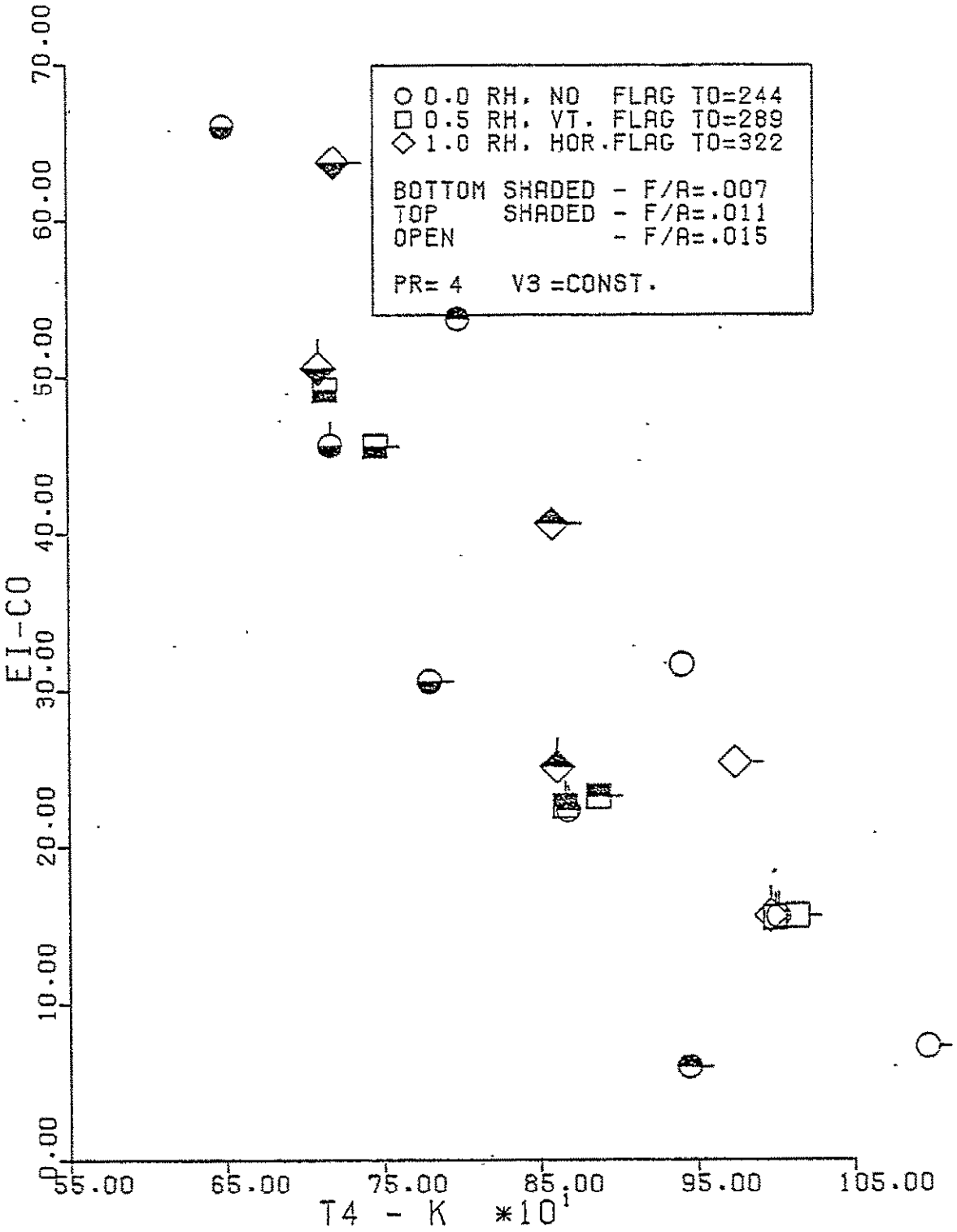

FIGURE 2. CARBON MONOXIDE EMISSION INDEX, JT8D-17.

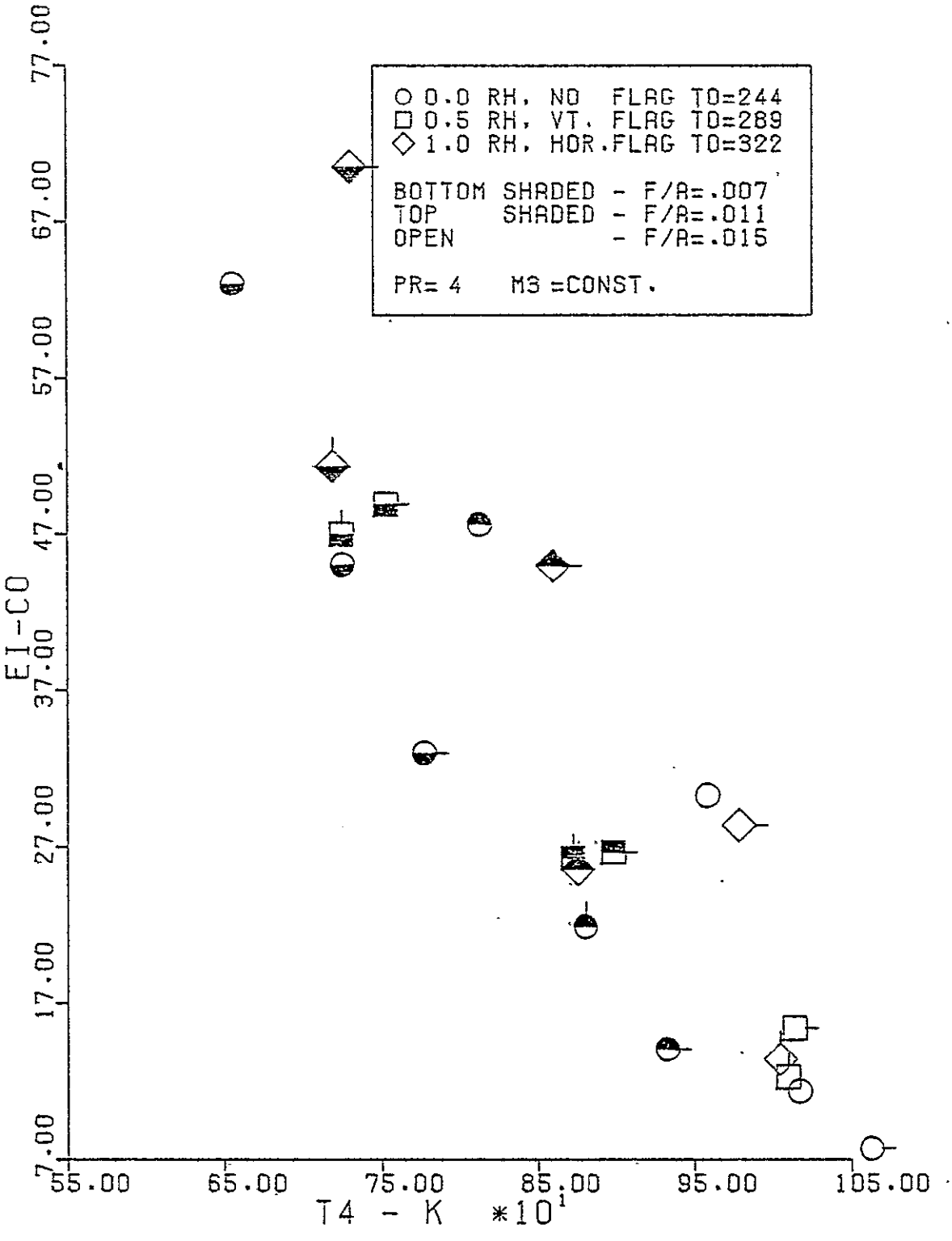

FIGURE 3. CARBON MONOXIDE EMISSION INDEX, JT8D-17.

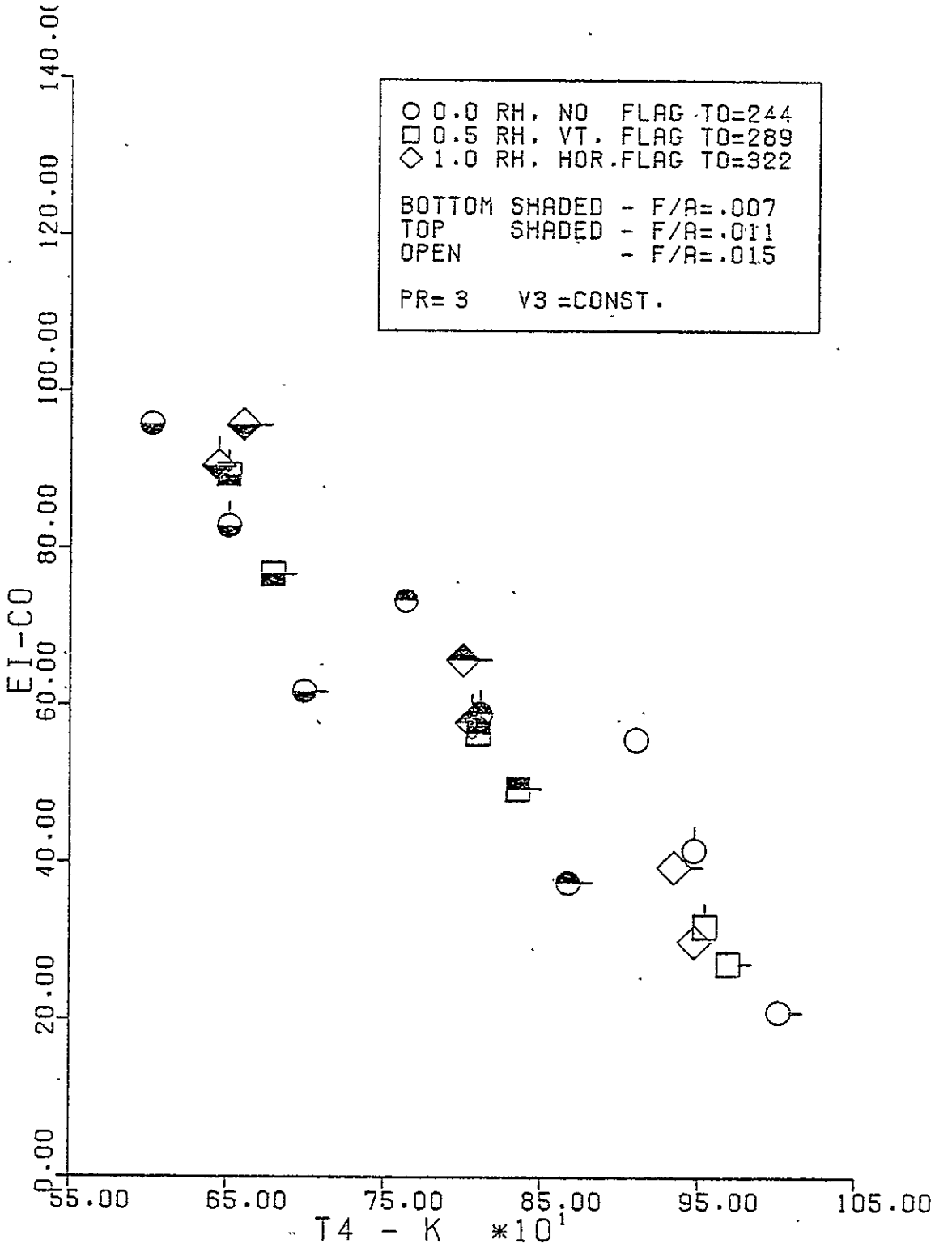

FIGURE 4. CARBON MONOXIDE EMISSION INDEX, JT8D-17.

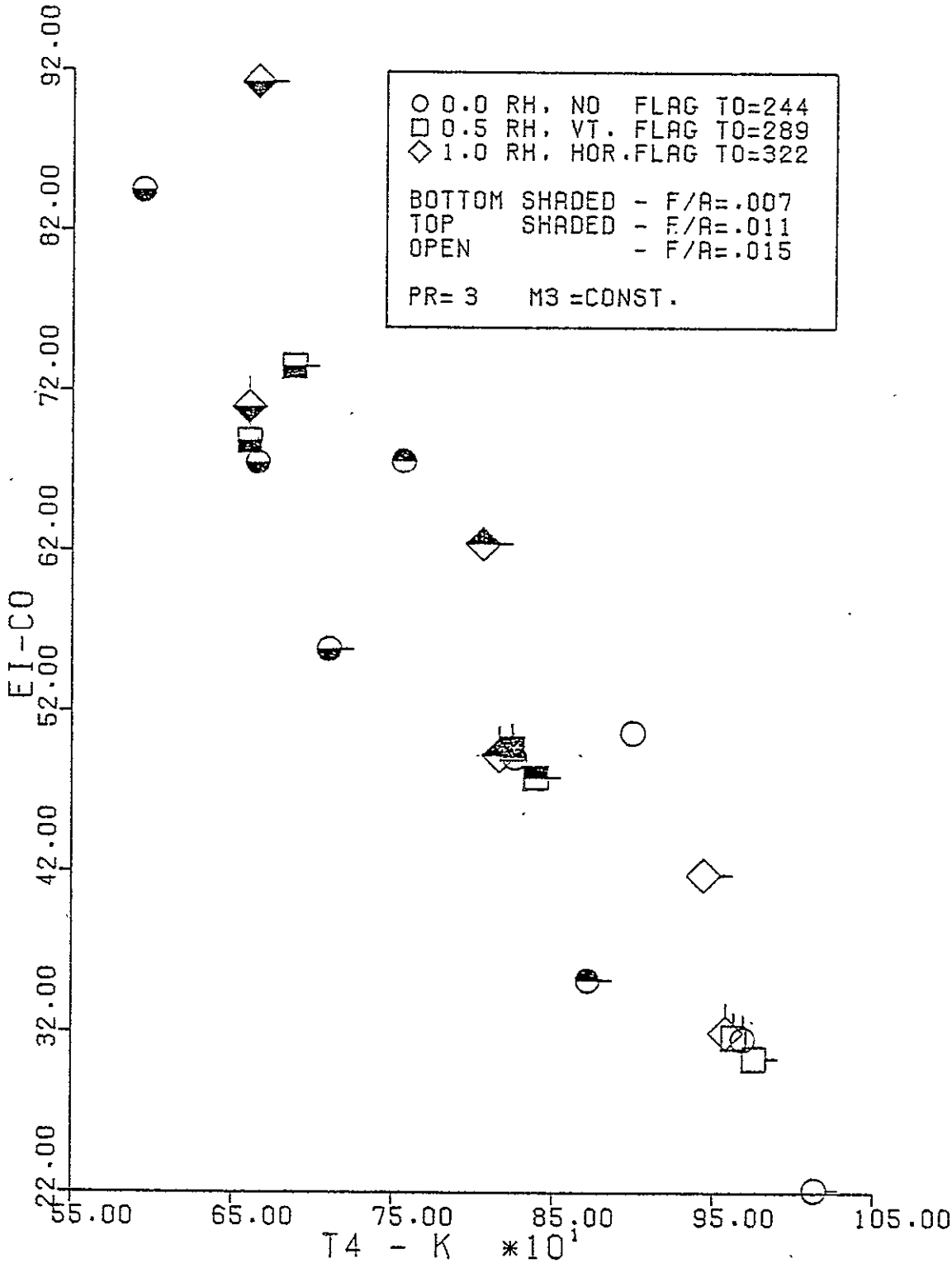

FIGURE 5. CARBON MONOXIDE EMISSION INDEX, JT8D-17.

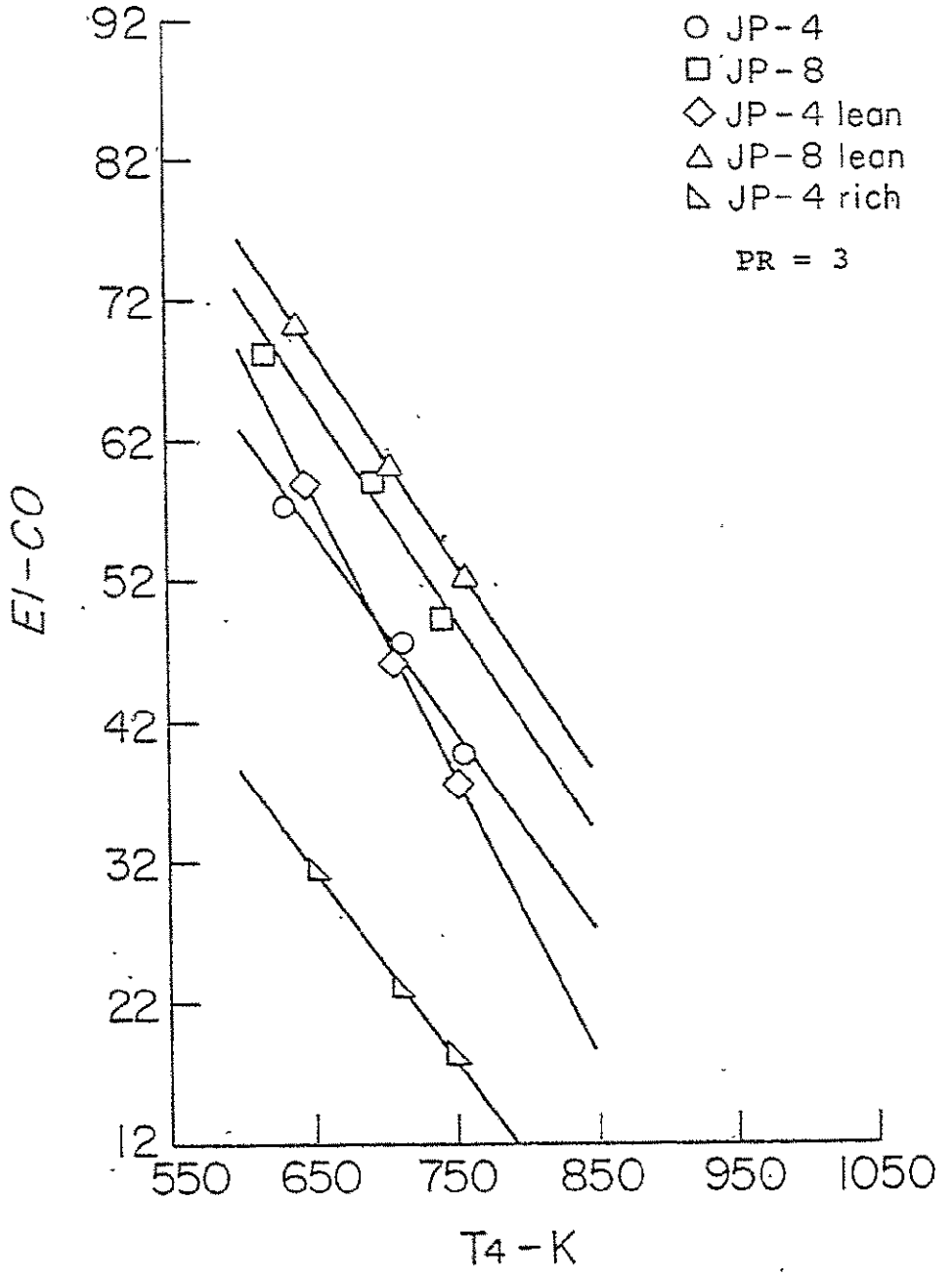

FIGURE 6. CARBON MONOXIDE EMISSION INDEX, T-56.

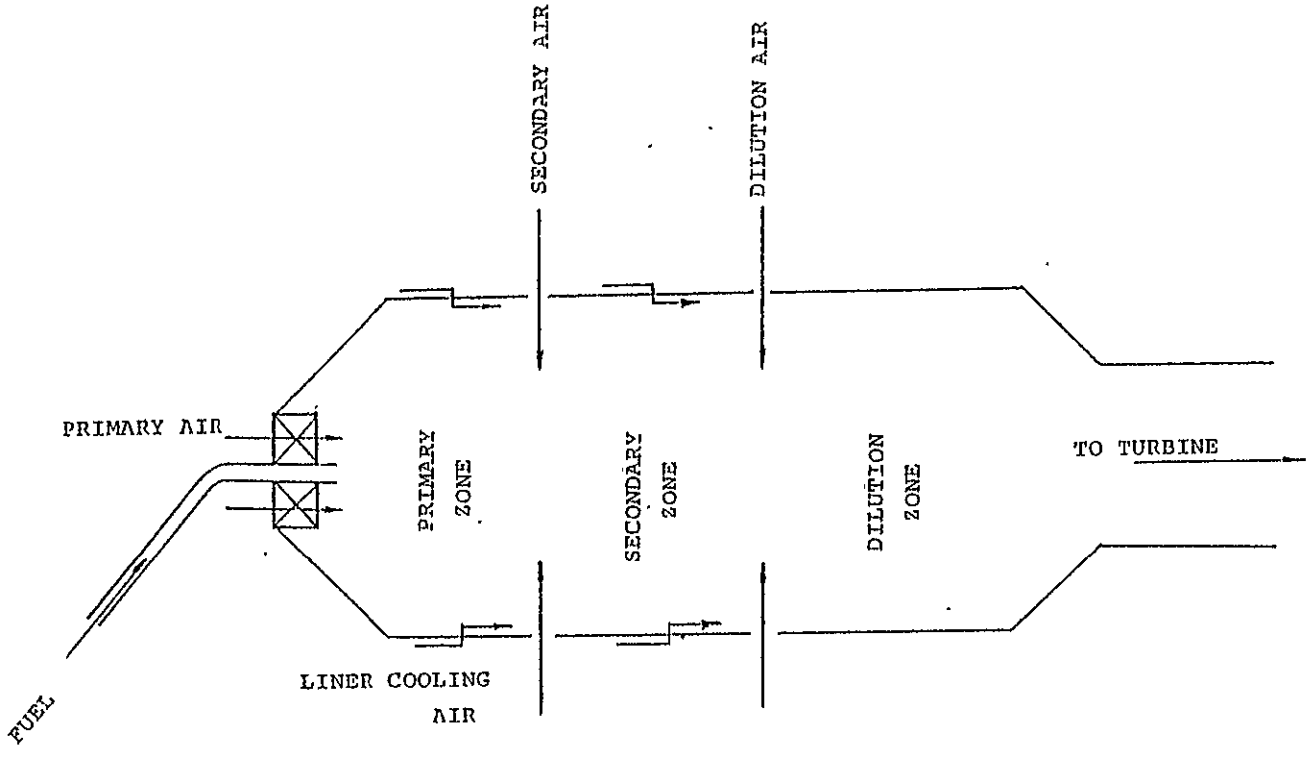

FIGURE 7. TYPICAL GAS TURBINE COMBUSTOR.

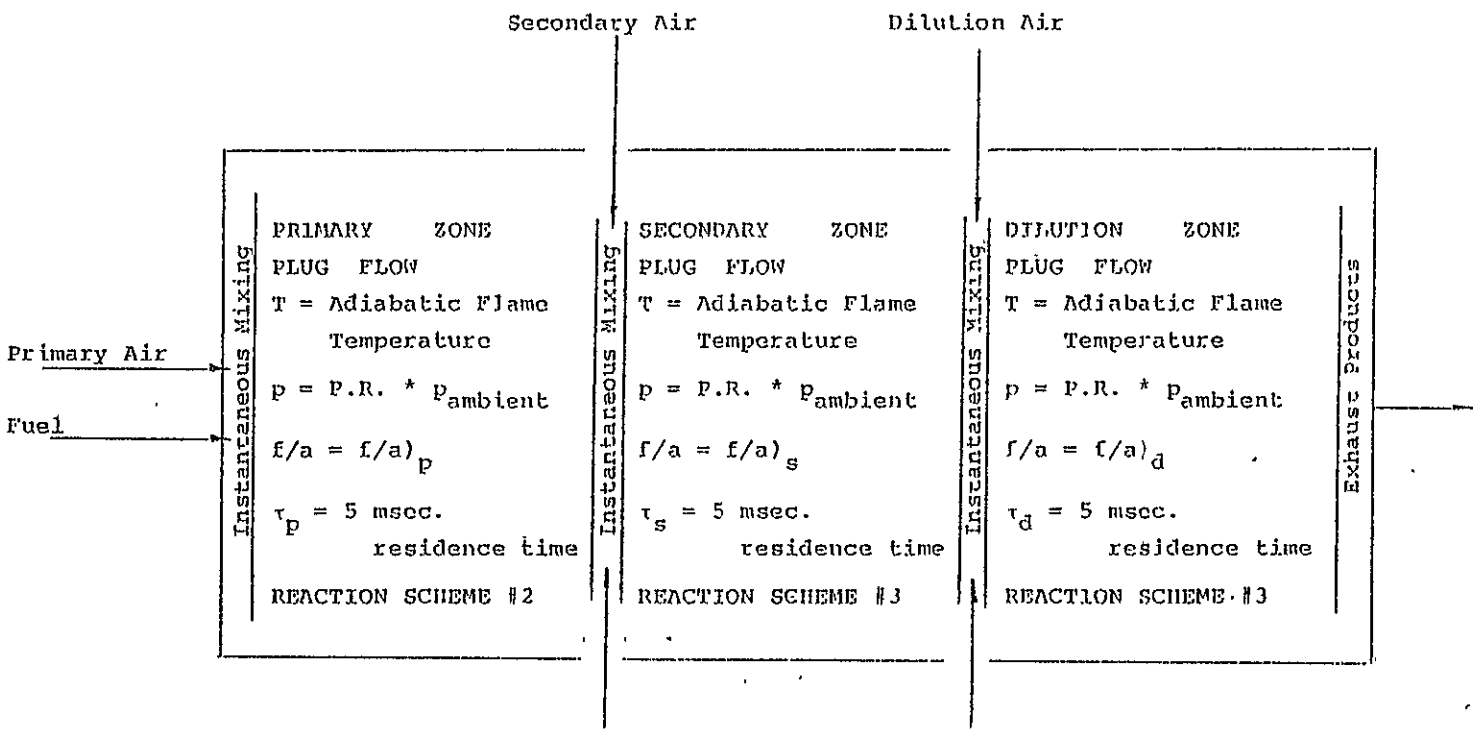

FIGURE 8. ANALYTICAL MODEL, RICH PRIMARY ZONE.

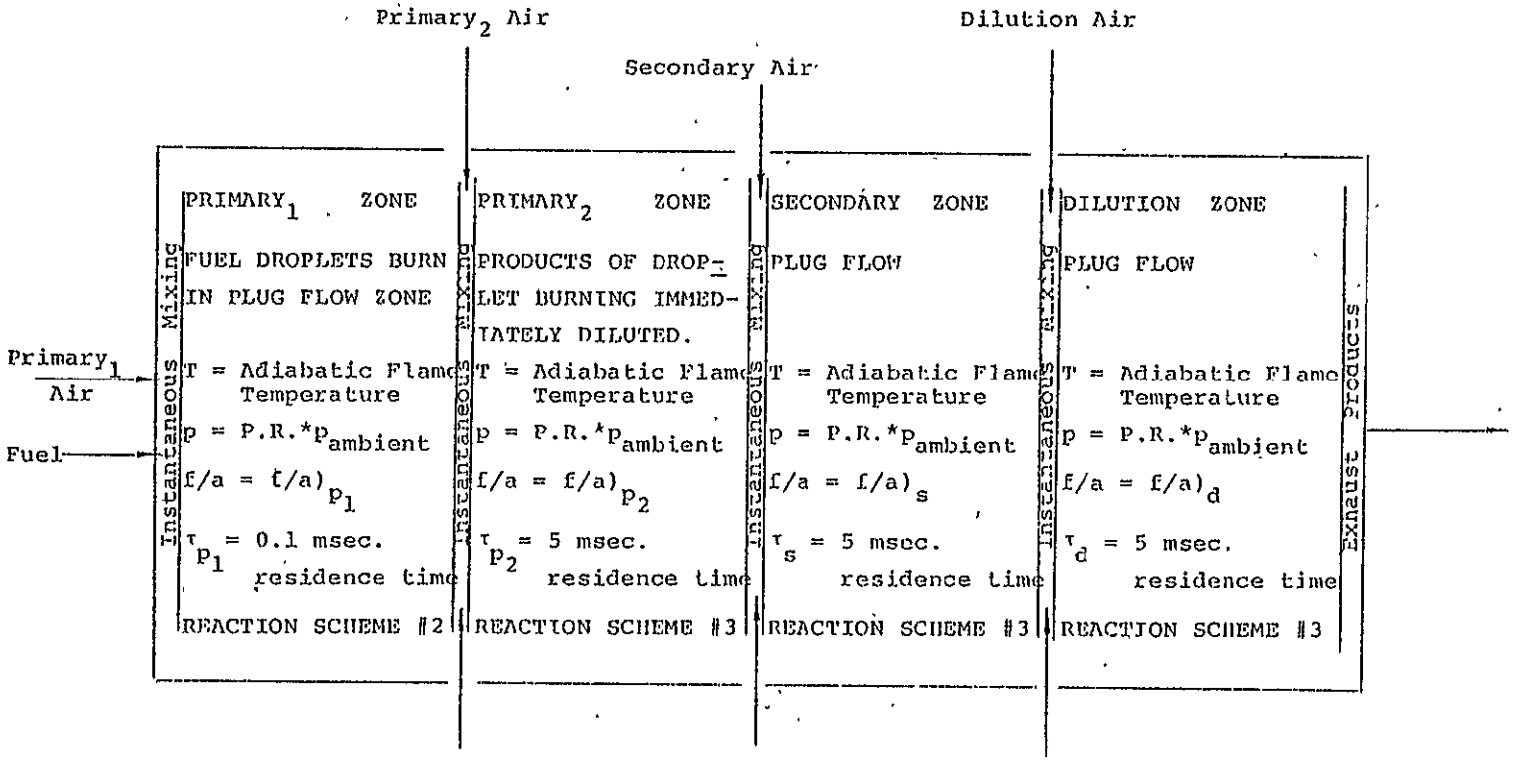

FIGURE 9. ANALYTICAL MODEL; LEAN PRIMARY ZONE.

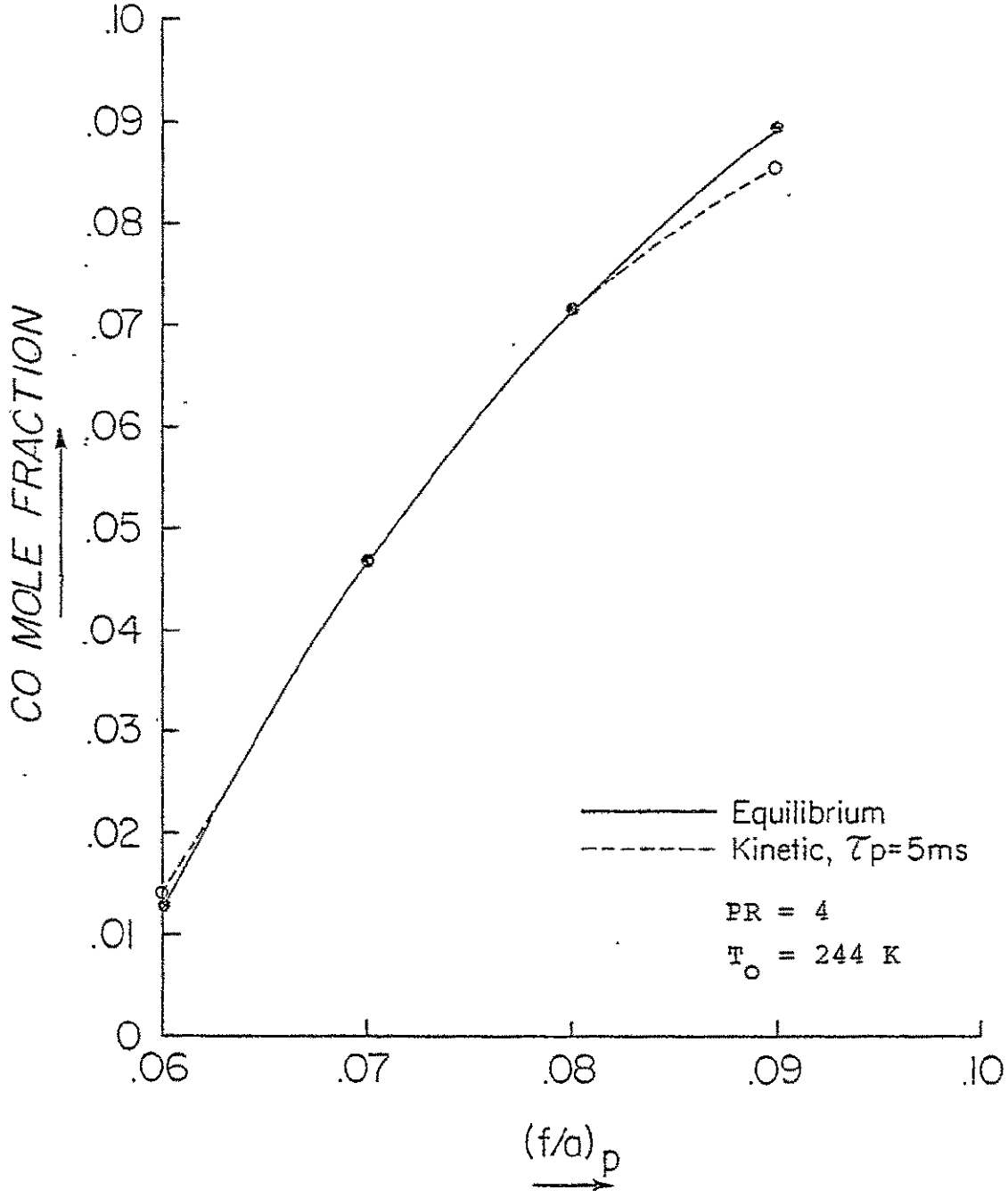

FIGURE 10. PRIMARY ZONE CARBON MONOXIDE LEVELS.

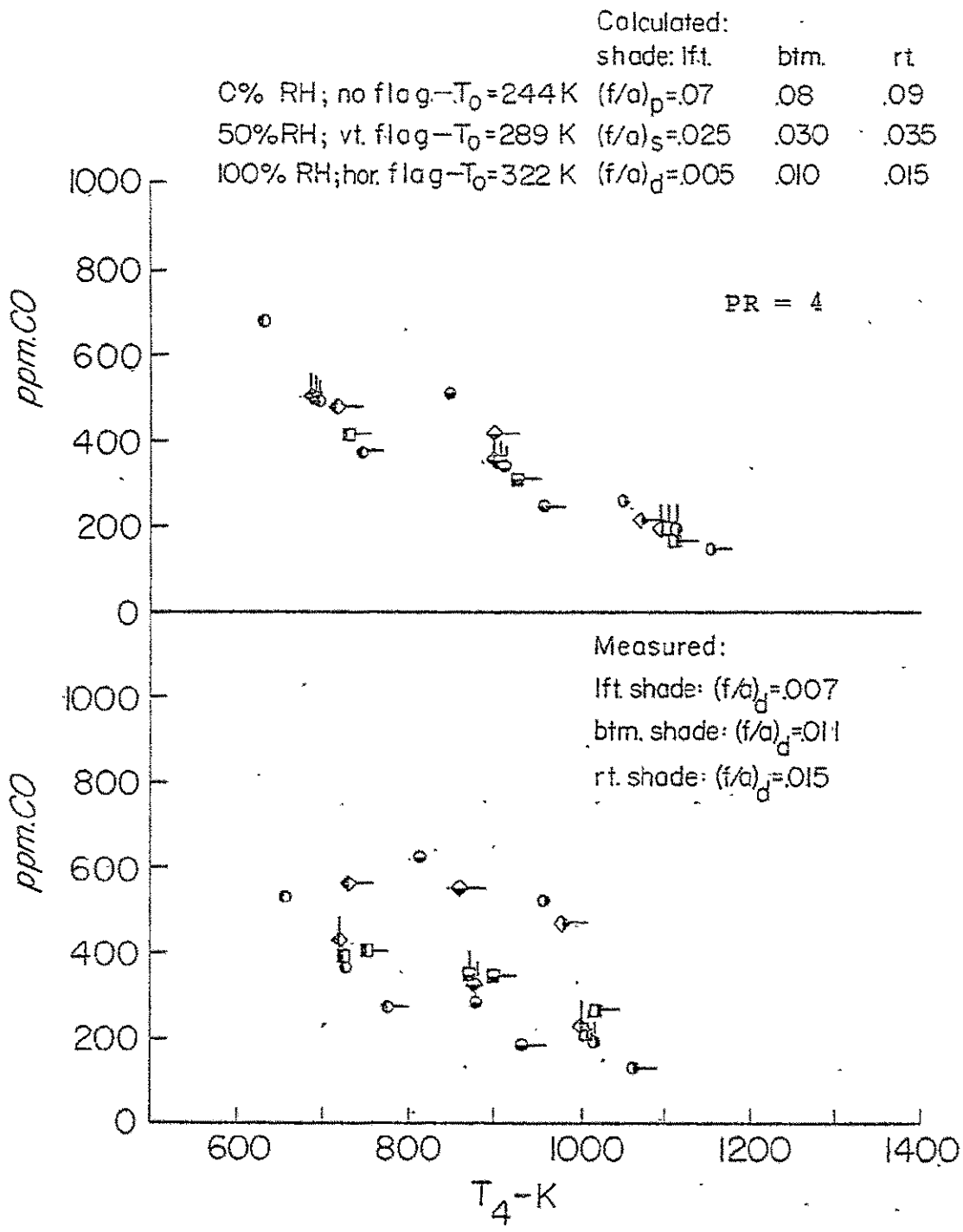

FIGURE 11. COMBUSTOR EXIT CARBON MONOXIDE LEVELS.

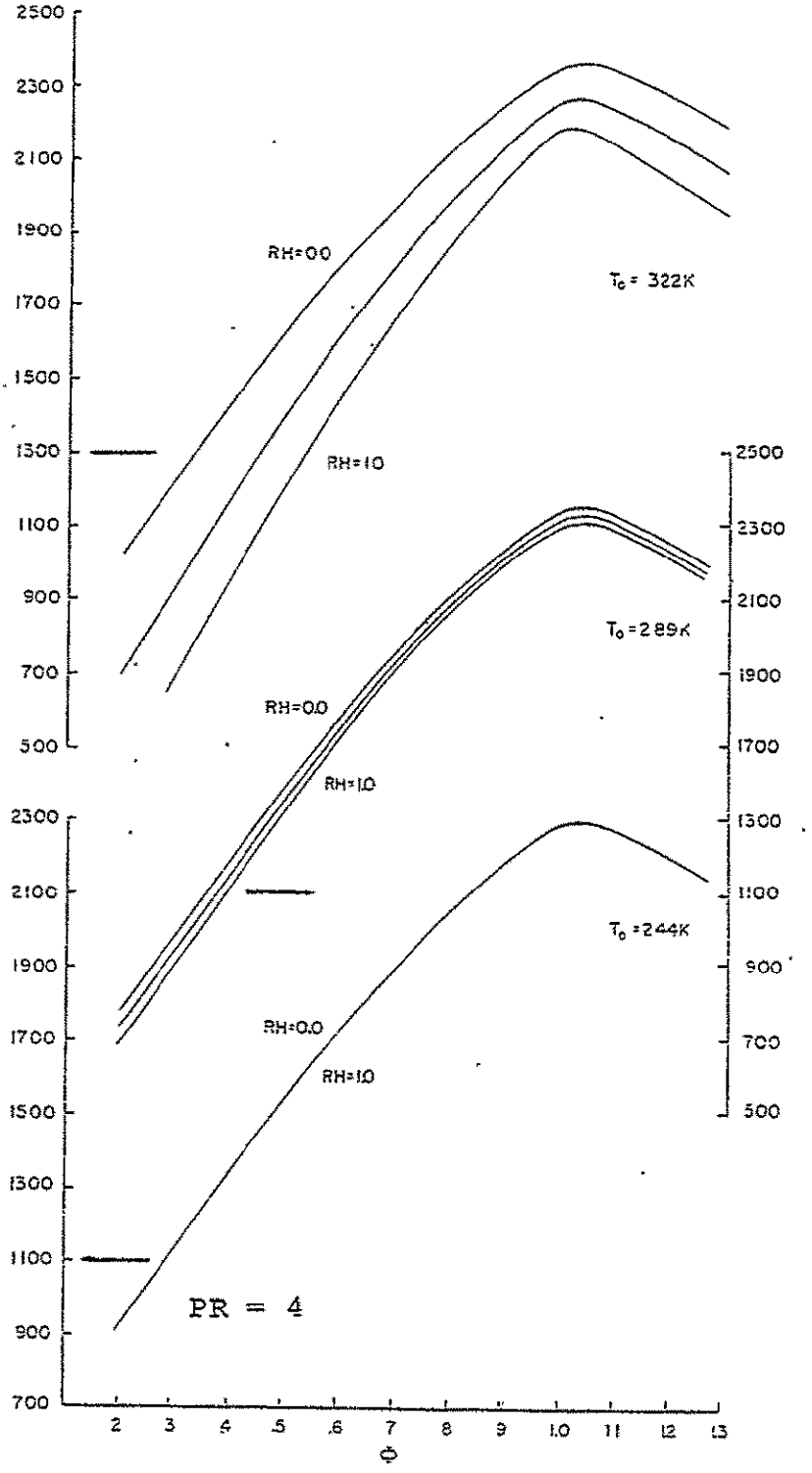

FIGURE 12. METHANE ADIABATIC FLAME TEMPERATURE.

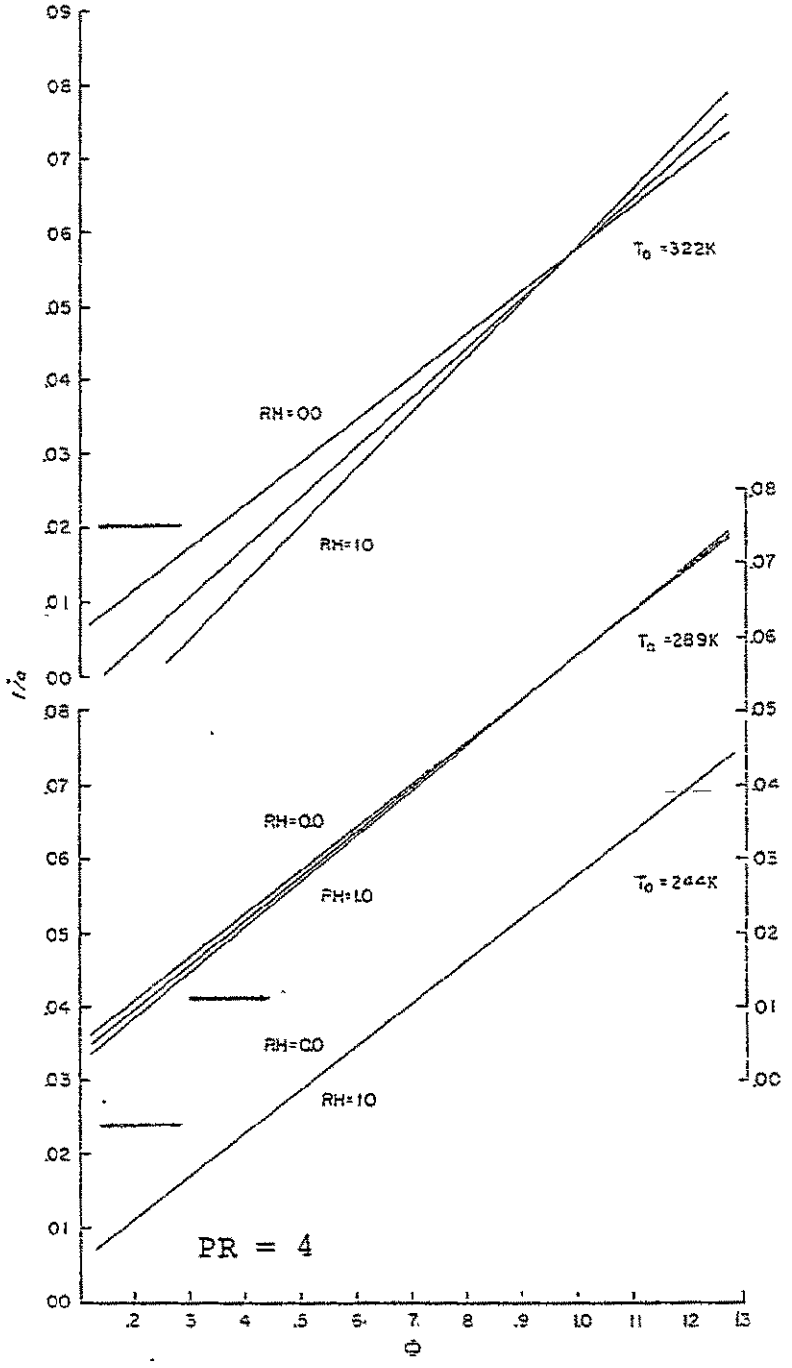

FIGURE 13. METHANE FUEL/AIR RATIO.

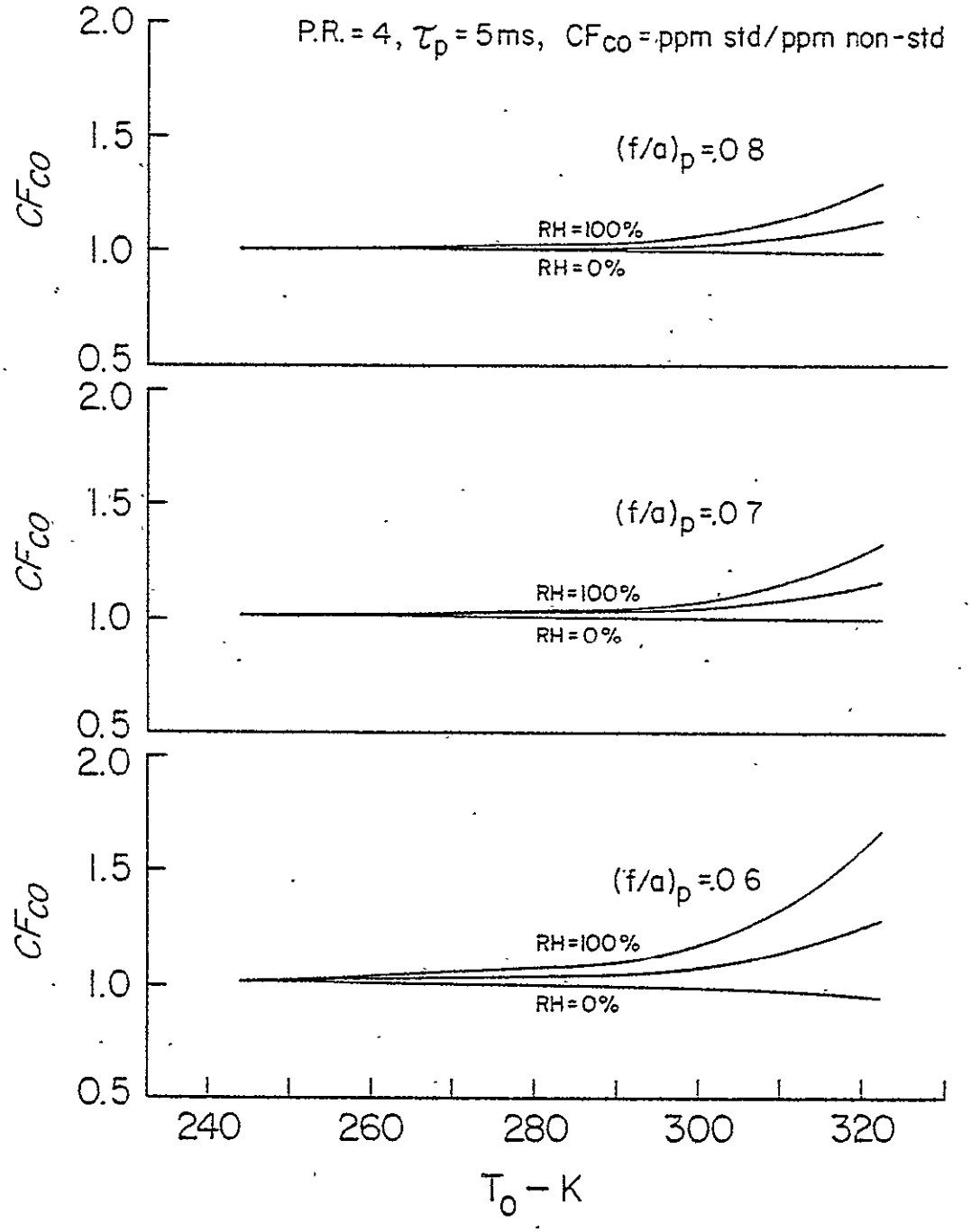

FIGURE 14. NORMALIZED PRIMARY ZONE CARBON MONOXIDE LEVELS, METHANE KINETIC SCHEME.

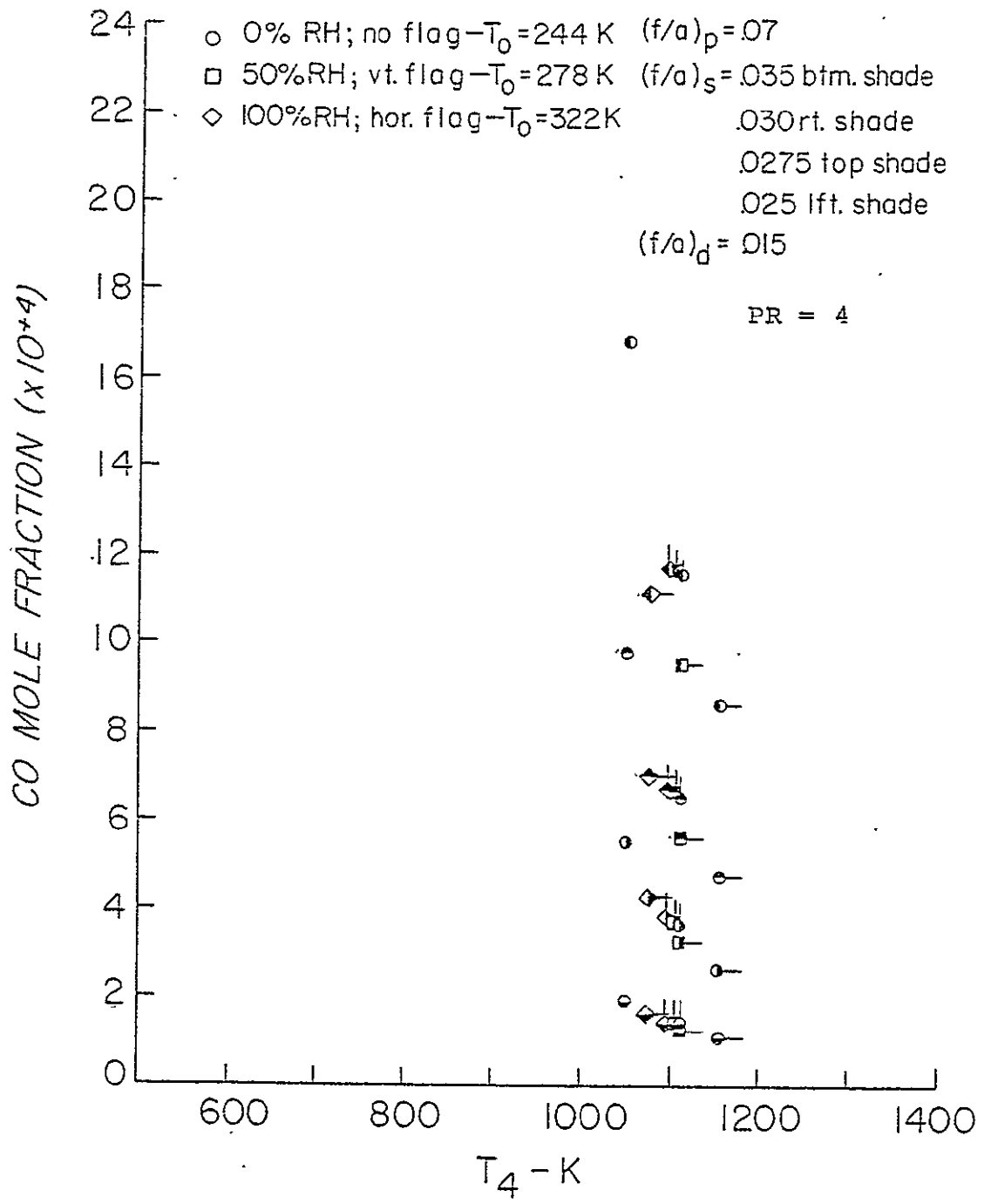

FIGURE 15. CARBON MONOXIDE EMISSIONS, METHANE KINETIC SCHEME.

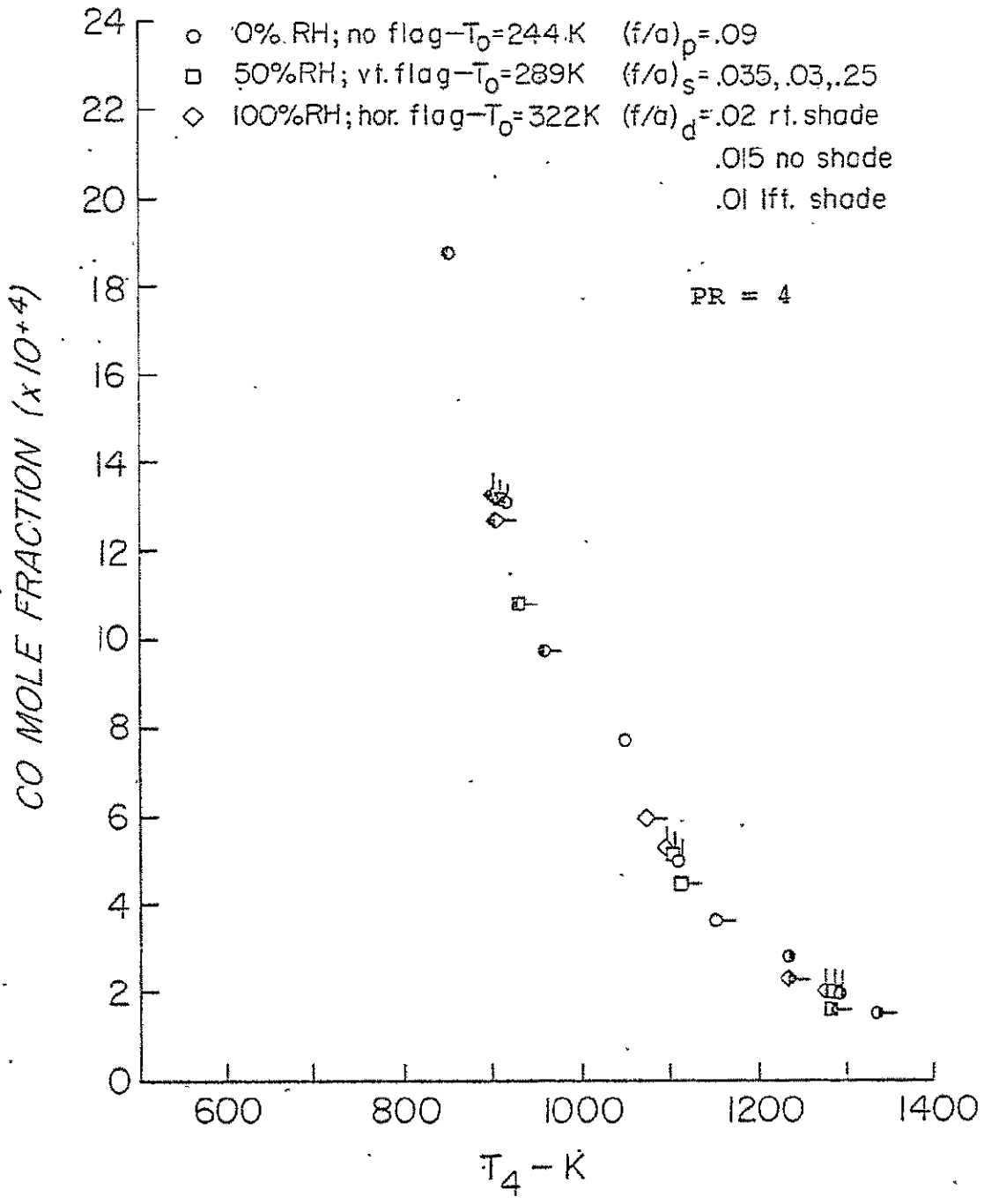

FIGURE 16. CARBON MONOXIDE EMISSIONS, METHANE KINETIC SCHEME.

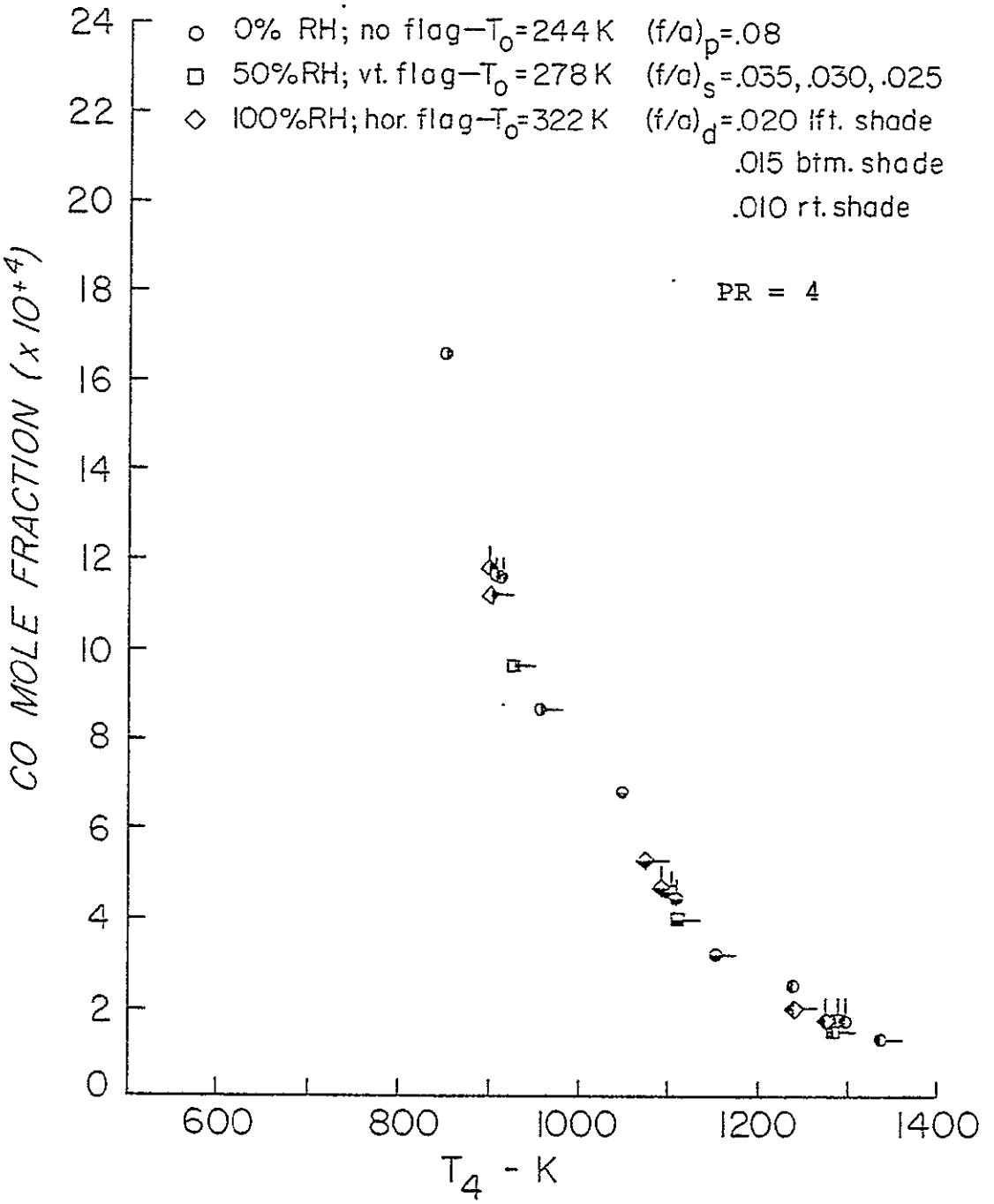

FIGURE 17. CARBON MONOXIDE EMISSIONS, METHANE KINETIC SCHEME.

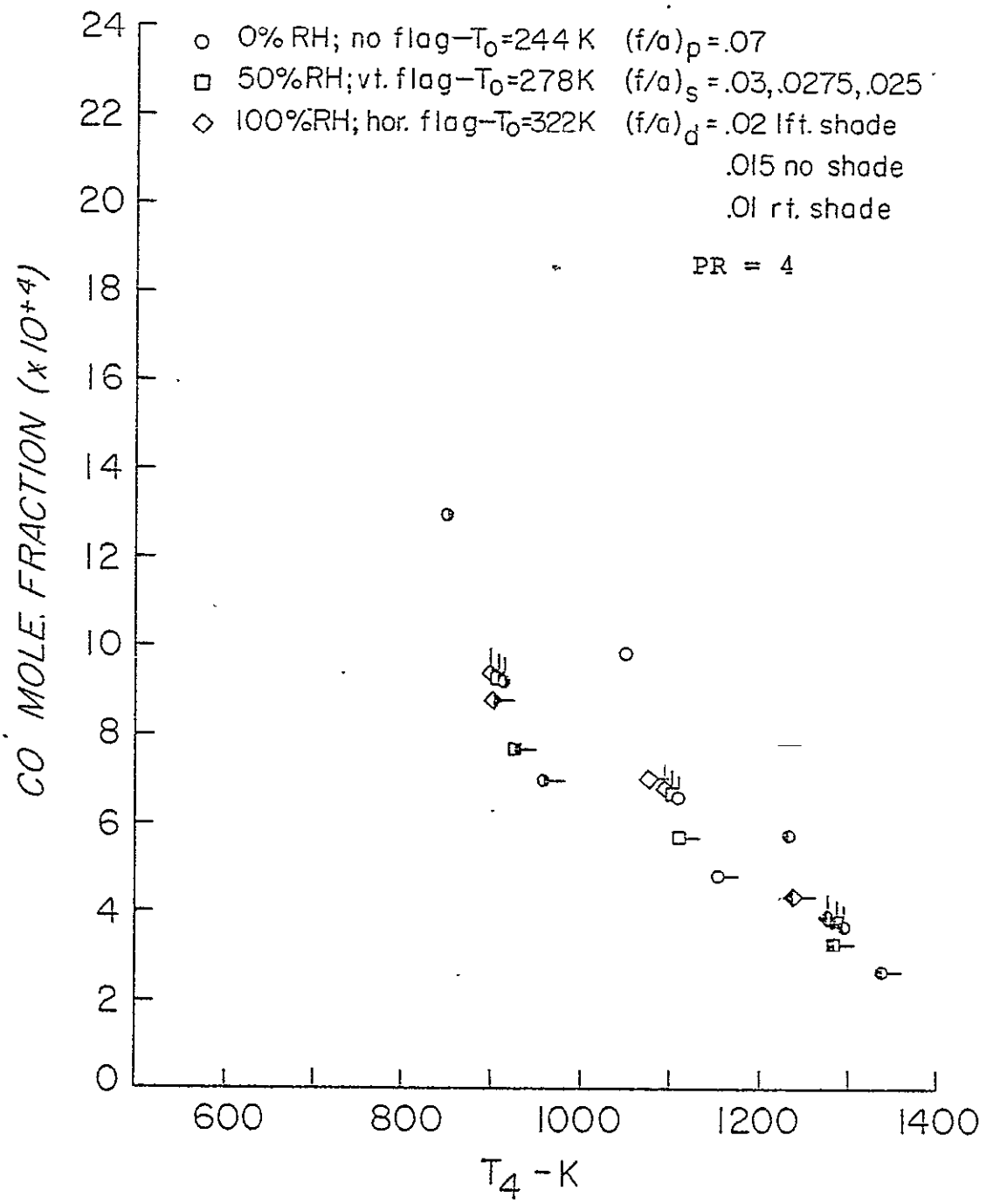

FIGURE 18. CARBON MONOXIDE EMISSIONS, METHANE KINETIC SCHEME.

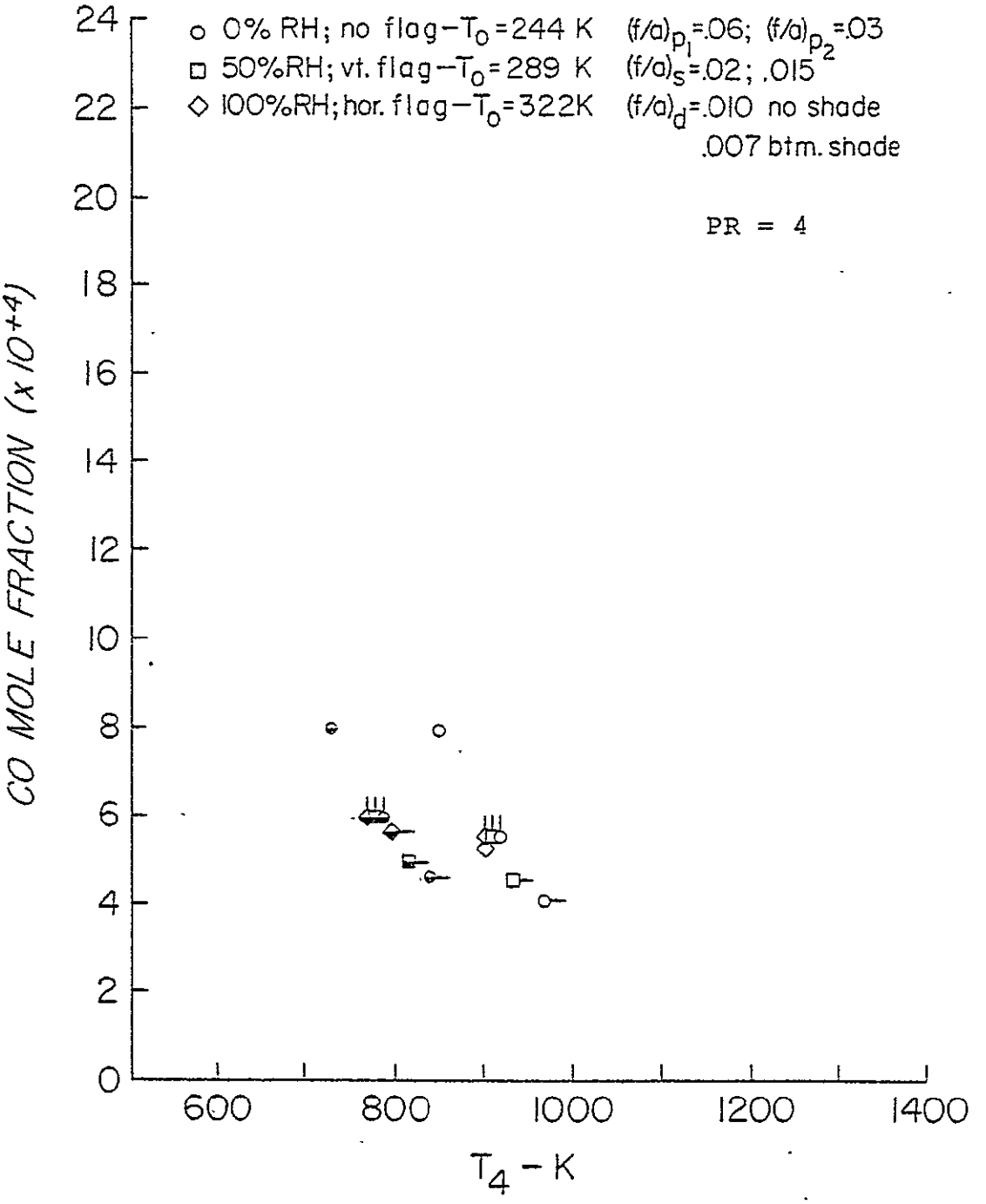

FIGURE 19. CARBON MONOXIDE EMISSIONS, METHANE KINETIC SCHEME.

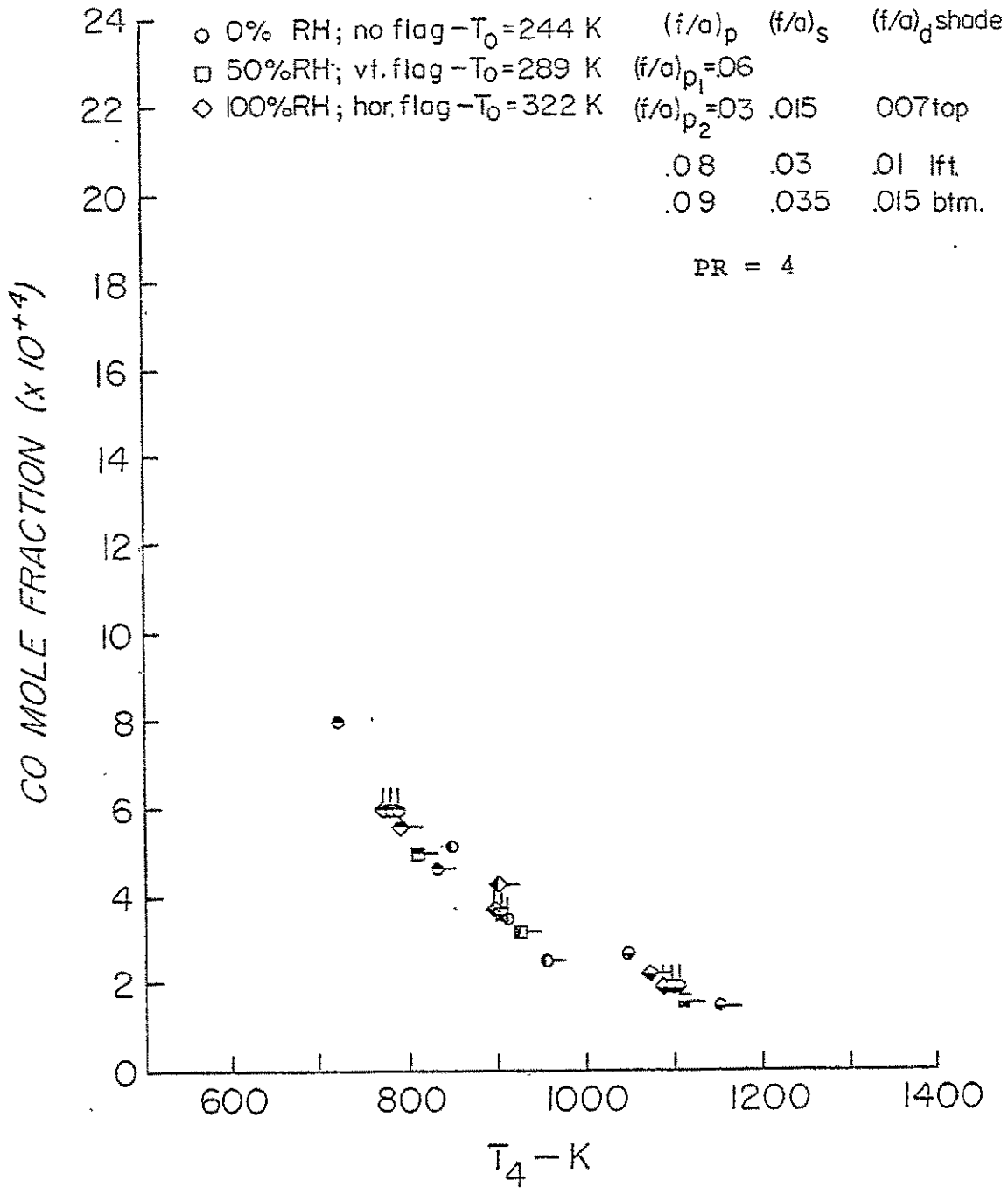

FIGURE 20. CARBON MONOXIDE EMISSIONS, METHANE KINETIC SCHEME.

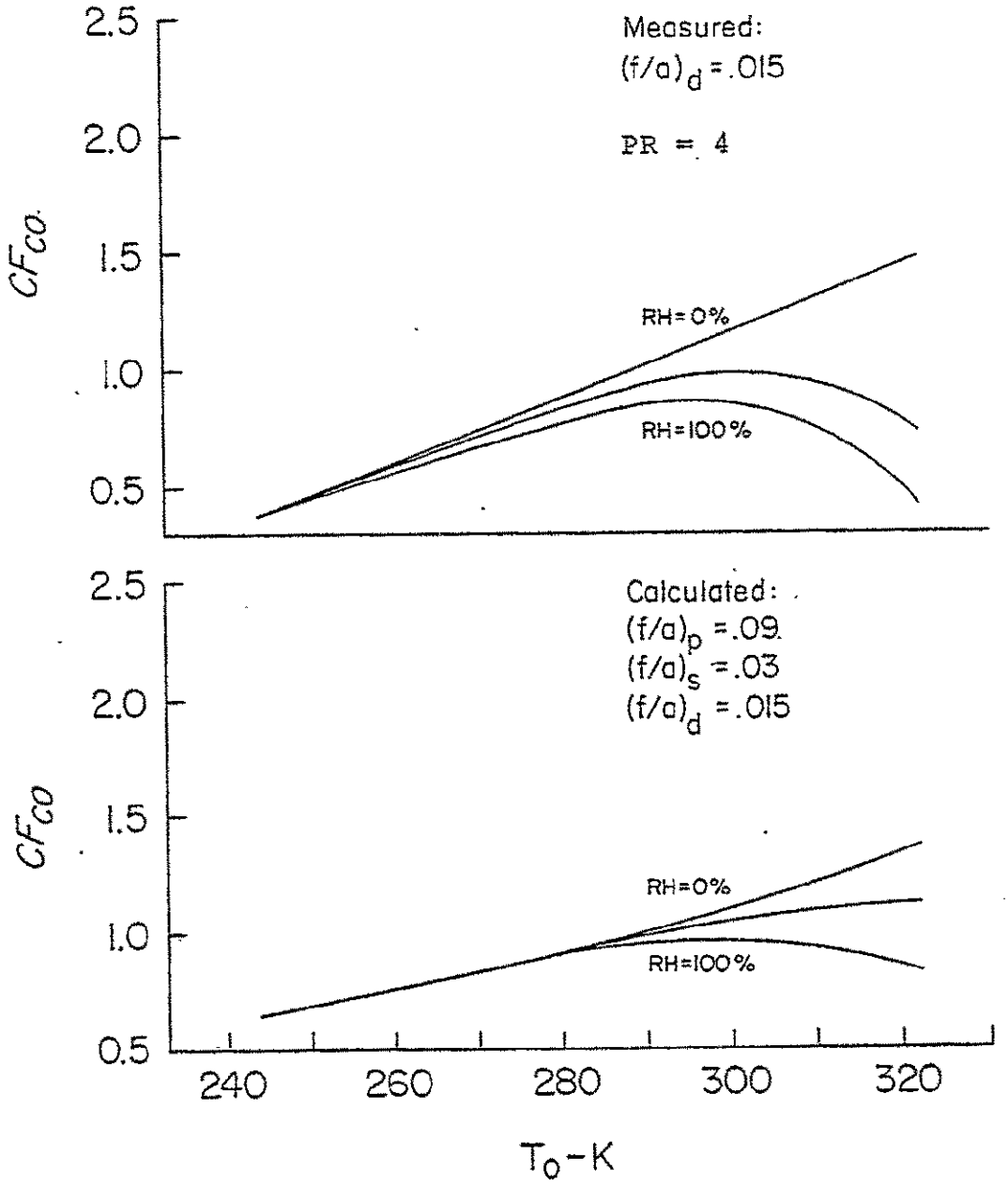

FIGURE 21. AMBIENT TEMPERATURE AND HUMIDITY CORRECTION FACTORS, JT8D-17.

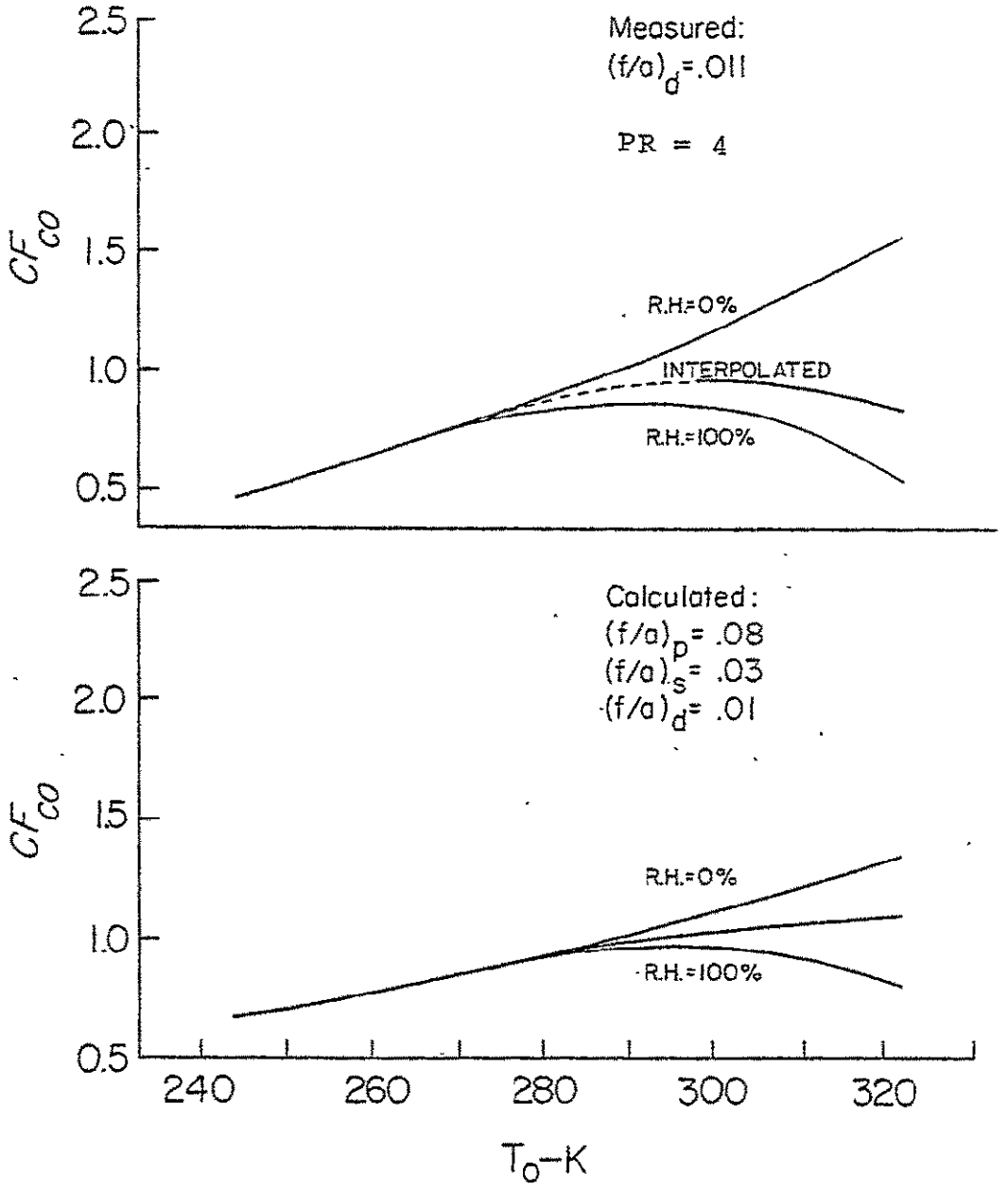

FIGURE 22. AMBIENT TEMPERATURE AND HUMIDITY CORRECTION FACTORS, JT8D-17.

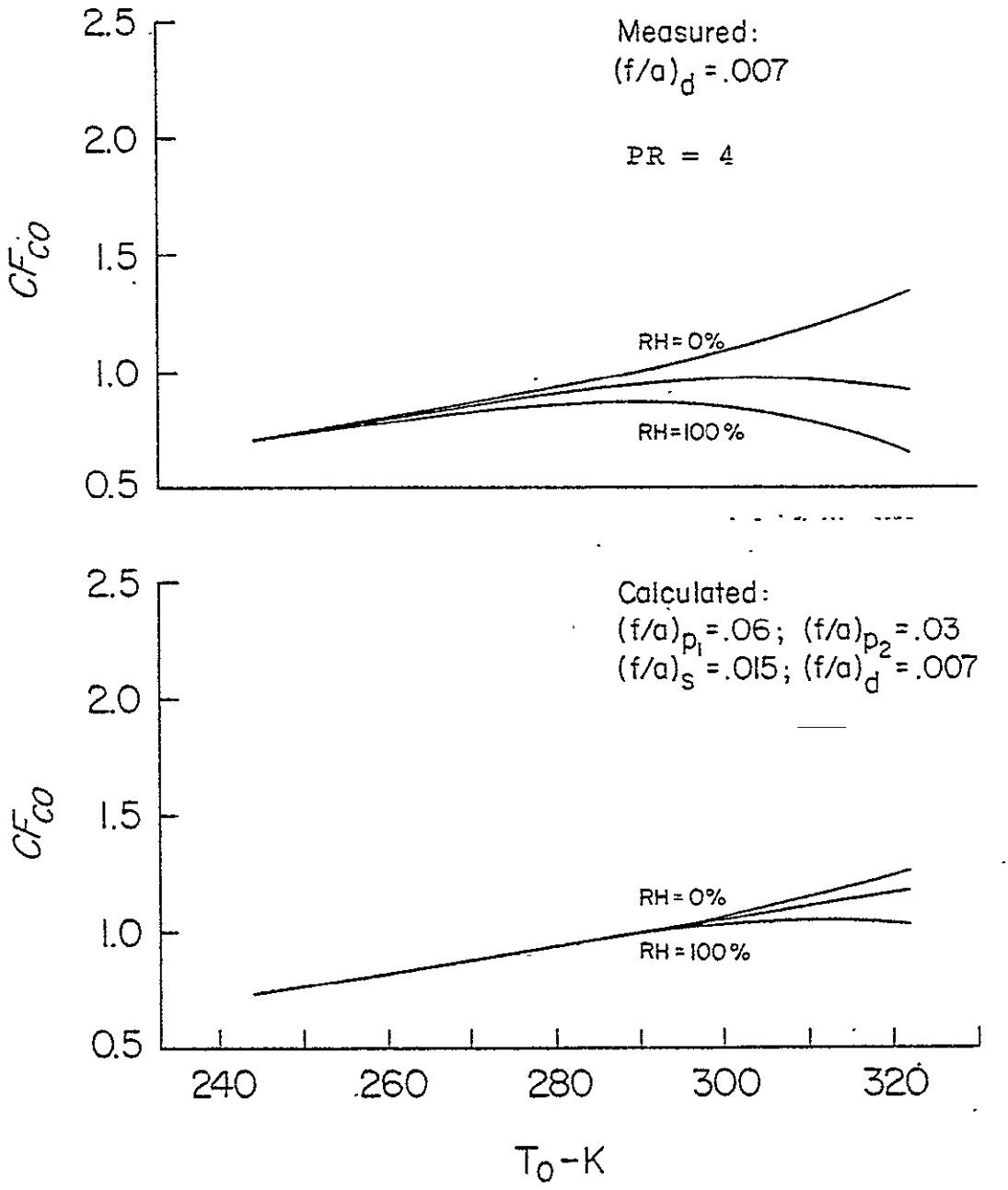

FIGURE 23. AMBIENT TEMPERATURE AND HUMIDITY CORRECTION FACTORS, JT8D-17.

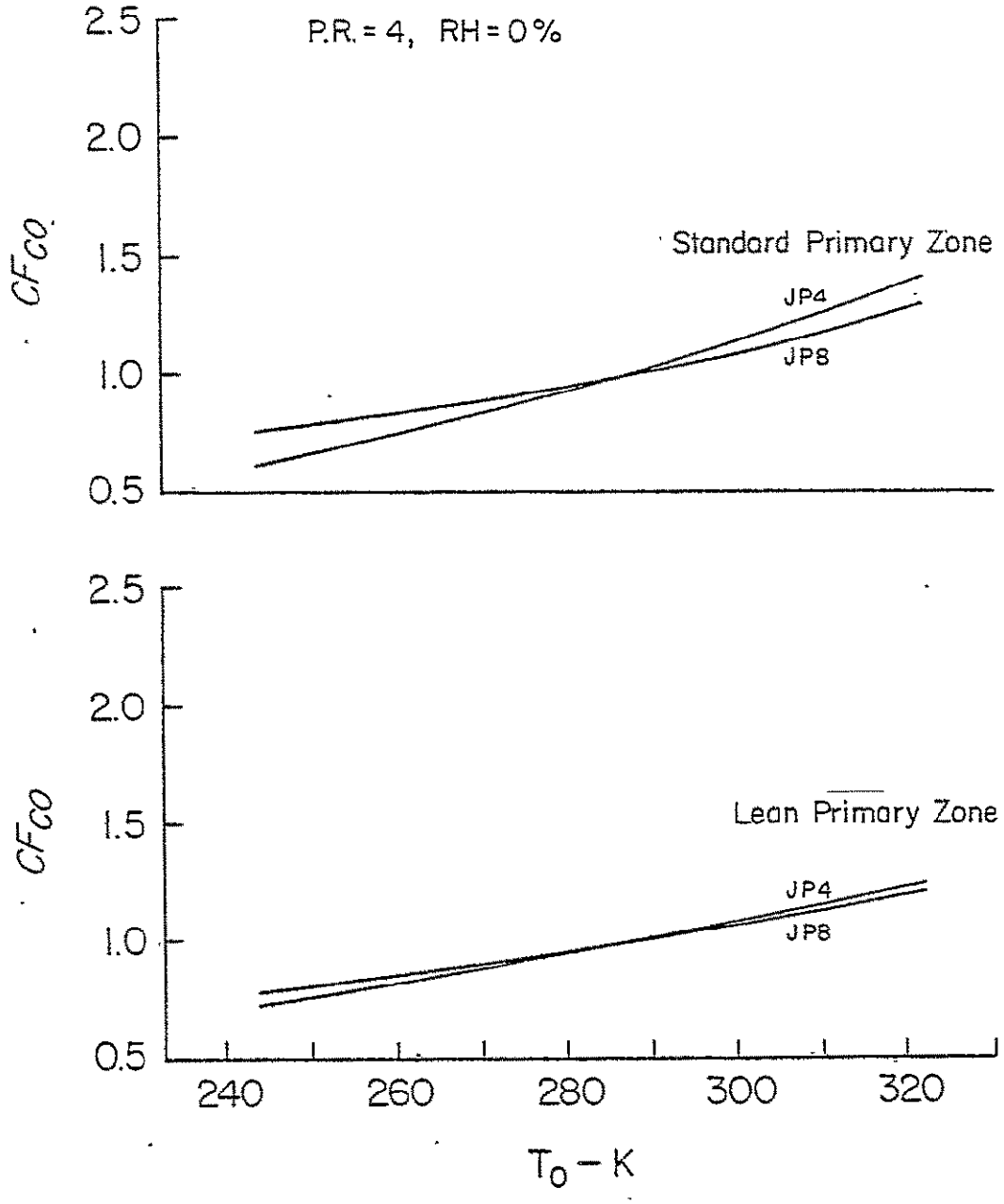

FIGURE 24. AMBIENT TEMPERATURE CORRECTION FACTORS, T-56.

TABLE I

IDLE JT8D - 17 COMBUSTOR CONDITIONS

Nominal Operation:

Total Inlet Pressure	2.47 atm.
Total Inlet Temperature	393 K
Air Flow	1.37 kg/sec
Fuel Flow	.0161 kg/sec
Fuel/Air Ratio	.0117

Test Conditions:

Compressor Efficiency	0.8
Compressor Pressure Ratio	2, 3, 4, 5
Compressor Inlet Pressure	1 atm.
Compressor Inlet Temperature	244, 289, 322 K
Compressor Inlet Relative Humidity	0, 50, 100 %
Fuel/Air Ratio	.015, .011, .007
Constant Compressor Discharge Mach Number	0.42, or,
Constant Reference Velocity	15.2 m/sec

TABLE II

Kinetic Scheme for Methane/Air Combustion With
Forward Rate Constants: $k_f = A\ T^{\alpha}\ e^{-\Delta E/RT}$
units: cm., mole, sec.

No.	Reaction	A	α	ΔE
1	$M + CH_4 = CH_3 + H + M$	0.20E18	0.0	88332.5
2	$CH_4 + OH = CH_3 + H_2O$	0.28E14	0.0	4962.5
3	$CH_4 + O = CH_3 + OH$	0.20E14	0.0	9210.4
4	$CH_4 + H = CH_3 + H_2$	0.69E14	0.0	11810.8
5	$CH_3 + O_2 = HCO + H_2O$	0.20E11	0.0	0.0
6	$CH_3 + O = HCO + H_2$	0.10E15	0.0	0.0
7	$HCO + OH = CO + H_2O$	0.10E15	0.0	0.0
8	$M + HCO = CO + H + M$	0.20E13	0.5	28584.0
9	$CO + OH = CO_2 + H$	0.56E12	0.0	600.0
		0.85E-14	7.0	-13895.0
10	$H + O_2 = O + OH$	0.22E15	0.0	16554.9
11	$O + H_2 = H + OH$	0.17E14	0.0	9428.8
12	$O + H_2O = OH + OH$	0.58E14	0.0	18004.0
13	$H + H_2O = H_2 + OH$	0.84E14	0.0	20048.5
14	$H + OH + M = H_2O + M$	0.40E20	-1.0	0.0
15	$H + H + M = H_2 + M$	0.15E19	-1.0	0.0
16	$O + O + M = O_2 + M$	0.40E18	-1.0	0.0
17	$O + H + M = OH + M$	0.53E16	0.0	5518.3
18	$N + O_2 = NO + O$	0.64E10	1.0	6232.9
19	$O + N_2 = NO + N$	0.14E15	0.0	75231.5
20	$OH + N = NO + H$	0.40E14	0.0	0.0
21	$O + CO_2 = CO + O_2$	0.19E14	0.0	54150.0

TABLE II (continued)

No.	Reaction	A	α	ΔE
22	$N_2 + O_2 = N + NO_2$	0.27E15	-1.0	120428.0
23	$N_2 + O_2 = NO + NO$	0.42E15	0.0	119100.0
24	$NO + NO = N + NO_2$	0.30E12	0.0	0.0
25	$M + NO = N + O + M$	2.27E17	-0.5	148846.0
26	$O + NO + M = NO_2 + M$	1.05E15	0.0	- 1870.0
27	$M + NO_2 = N + O_2 + M$	6.00E14	-1.5	105200.0
28	$O + NO_2 = NO + O_2$	1.00E13	0.0	600.0
29	$H + NO_2 = NO + OH$	7.25E14	0.0	1930.0
30	$N + CO_2 = CO + NO$	2.00E11	-0.5	7950.0
31	$CO + NO_2 = NO + CO_2$	2.00E11	-0.5	4968.0

TABLE II a

REACTION SCHEMES

Scheme:	Reactions:
1	All reactions in Table II except reaction 6.
2	The first 20 reactions in Table II, with the first given rate constant for reaction 9.
3	The first 20 reactions in Table II, with the second given rate constant for reaction 9.

TABLE III

LOCAL FUEL/AIR RATIOS AND RESIDENCE TIMES

TYPICAL COMBUSTOR:

	Primary		Secondary		Dilution	
	High	Low	High	Low	High	Low
Fuel/Air Ratio	.071	.048	.034	.019	.012	.011
Residence Time (milliseconds)	1.90	1.60	4.47	3.54	2.62	2.45

ANALYTICAL MODEL:

	Primary	Secondary		Dilution	
		High	Low	High	Low
Fuel/Air Ratio	.07	.035	.025	.020	.010
Residence Time (milliseconds)	5.0	5.0	5.0	5.0	5.0

TABLE IV

EQUILIBRIUM CARBON MONOXIDE MOLE FRACTION AND ADIABATIC FLAME TEMPERATURE DEG K

PR = 4 METHANE FUEL

Equivalence Ratio		1.2	1.0	0.8	1.2	1.0	0.8
T_o K	RH %	Equilibrium Carbon Monoxide			Adiabatic Flame Temperature		
244	0	.04548	.00795	.00043	2196	2298	2059
244	50	.04548	.00794	.00042	2196	2298	2059
244	100	.04547	.00793	.00042	2196	2298	2058
289	0	.04584	.00904	.00060	2238	2331	2103
289	50	.04563	.00854	.00050	2221	2319	2083
289	100	.04541	.00807	.00042	2204	2307	2064
322	0	.06169	.00991	.00076	2269	2355	2136
322	50	.04448	.00662	.00022	2151	2269	1998
322	100	.04268	.00440	.00006	2045	2190	1872

TABLE IV Cont'd.

EQUILIBRIUM CARBON MONOXIDE MOLE FRACTION AND ADIABATIC FLAME TEMPERATURE

PR = 4 JP 4 FUEL

Equivalence Ratio		1.2	1.0	0.8	1.2	1.0	0.8
T_o K	RH %	Equilibrium Carbon Monoxide			Adiabatic Flame Temperature		
244	0	.05948	.01284	.00091	2280	2354	2118
244	50	.05948	.01283	.00090	2280	2354	2118
244	100	.05948	.01281	.00090	2279	2354	2117
289	0	.05988	.01442	.00125	2322	2386	2162
289	50	.05972	.01367	.00106	2304	2373	2141
289	100	.05955	.01295	.00089	2287	2361	2121
322	0	.06022	.01567	.00156	2353	2409	2194
322	50	.05886	.01069	.00047	2229	2322	2050
322	100	.05722	.00725	.00013	2117	2241	1918

TABLE V

RATE CONSTANTS FOR THE $CO + OH = CO_2 + H$ REACTION

T,Deg. Kelvin	Large K	Used K	Small K
500.00	.22833E10	.79860E11	.11892E10
600.00	.12863E11	.27749E11	.30957E10
700.00	.44221E11	.15419E11	.61311E10
800.00	.11165E12	.11249E11	.10236E11
900.00	.22944E12	.97043E10	.15249E11
1000.0	.40826E12	.93214E10	.20977E11
1100.0	.65419E12	.96130E10	.27230E11
1200.0	.96903E12	.10401E11	.33844E11
1300.0	.13512E13	.11629E11	.40680E11
1400.0	.17967E13	.13298E11	.47629E11
1500.0	.23000E13	.15444E11	.54604E11
1600.0	.28548E13	.18126E11	.61541E11
1700.0	.34546E13	.21421E11	.68389E11

TABLE VI

CORRECTION FACTORS, CARBON MONOXIDE, T 56 COMBUSTOR

PR = Pressure Ratio T_o = Ambient Temperature

Primary Zone	Fuel	Correction Factor
Std.	JP 4	$.970772 - .045481*PR + .001057*PR*T_o$
Std.	JP 8	$1.031017 - .05713*PR + .000843*PR*T_o$
Lean	JP 4	$1.030849 - .059991*PR + .000961*PR*T_o$
Lean	JP 8	$1.027965 - .050659*PR + .000737*PR*T_o$

APPENDIX 1

PROGRAM FOR COMPUTING MASS FRACTIONS AT PRIMARY ZONE INLET PRINTED AND PUNCHED OUTPUT

```
      IMPLICIT REAL*8 (A-H,N,O-Z)
      NAMELIST/PRIMA/FBA,WS,RH,T
      DO 111 KKK=1,9
      READ(5,PRIMA)
      WRITE(6,PRIMA)
      N2=0.7555D0
      O2=.2313D0
      AR=.0127D0
      CO2=.0005D0
      AIR=N2+O2+AR+CO2
      H2O=AIR*WS*RH
      FUEL=AIR*FBA
      SUM=AIR+H2O+FUEL
      N2=N2/SUM
      O2=O2/SUM
      AR=AR/SUM
      CO2=CO2/SUM
      H2O=H2O/SUM
      FUEL=FUEL/SUM
      CH4=FUEL
      IF(DABS(RH-0.0D0).LE.1.0D-10) GO TO 2
      WRITE(6,100)N2,O2,AR,CO2,H2O,CH4,T
      WRITE(7,100)N2,O2,AR,CO2,H2O,CH4,T
      GO TO 111
    2 WRITE(6,200)N2,O2,AR,CO2,CH4,T
      WRITE(7,200)N2,O2,AR,CO2,CH4,T
  100 FORMAT(1X,'N2=',D11.5,',O2=',D11.5,',AR=',D11.5,',',/,
     11X,'CO2=',D11.5,',H2O=',D11.5,',CH4=',D11.5,',T=',F6.1,
     2'   &END')
  200 FORMAT(1X,'N2=',D11.5,',O2=',D11.5,',AR=',D11.5,',',/,
     11X,'CO2=',D11.5,',CH4=',D11.5,',T=',F6.1,'   &END')
  111 CONTINUE
      STOP
      END
```

APPENDIX 2

PROGRAM FOR COMPUTING MASS FRACTIONS AT SECONDARY OR DILUTION INLET PROGRAM GIVES BOTH PRINTED AND PUNCHED OUTPUT

```
C          1     2     3     4     5     6     7     8     9     10
C        CH4   CH3     H    OH    H2O     O    H2    O2   HCO    CO
C
C          11    12    13    14    15    16
C         CO2     N    NO    N2    AR   NO2
      IMPLICIT REAL*8 (A-H,N,O-Z)
      DIMENSION COMPI(20),COMPD(20),COMPT(20),COMPE(20)
C                                   INPUT     CONDITIONS
      NAMELIST/XINP/WS,RH,FBOO,FBOP,T
      M=15
C
      DO 111 KKK=1,9
      READ(5,XINP)
      OXO=1.0D0/FBOO
      OXP=1.0D0/FBOP
      OXD=OXO-OXP
C  COMPUTE MASS FRACTIONS OF FRESH AIR WITH HUMIDITY
C     INITIALIZE ALL COMPONENTS TO ZERO
      DO 111 I=1,M
  111 COMPI(I)=0.0D0
      COMPI(8)=.2313D0
      COMPI(11)=.0005D0
      COMPI(14)=.7555D0
      COMPI(15)=.0127D0
      COMPI(5)=RH*WS
      ADD=COMPI(5)+COMPI(8)+COMPI(11)+COMPI(14)+COMPI(15)
      COMPI(5)=COMPI(5)/ADD
      COMPI(8)=COMPI(8)/ADD
      COMPI(11)=COMPI(11)/ADD
      COMPI(14)=COMPI(14)/ADD
      COMPI(15)=COMPI(15)/ADD
```

```
C COMPUTE MASSES OF COMPONENTS IN DILUTION AIR ---- COMPD(I)
      DO 222 JJ=1,M
  222 COMPD(JJ)=COMPI(JJ)*OXD
C     READ 10000,(COMPT(I),I=1,M)
      PRINT 30000,(COMPT(I),I=1,M),T
      DO 223 K=1,M
  223 COMPT(K)=COMPT(K)*(OXP+1.0D0)
      DO 333 K=1,M
  333 COMPE(K)=COMPD(K)+COMPT(K)
      SUM=0.000
      DO 444 L=1,M
  444 SUM=SUM+COMPE(L)
      DO 555 LL=1,M
  555 COMPE(LL)=COMPE(LL)/SUM
      WRITE(6,XINP)
C     PRINT 30000,(COMPE(I),I=1,M),T
      WRITE(7,12345)(COMPE(I),I=1,M),T
10000 FORMAT(7D11.5,3X)
12345 FORMAT(1X,'CH4=',D15.7,',CH3=',D15.7,',H=',D15.7,',OH=
     *',D15.7,',',
     1/,1X,'H2O=',D15.7,',O=',D15.7,',H2=',D15.7,',O2=',D15.
     *7,',',/,1X,'
     2HCO=',D15.7,',CO=',D15.7,',CO2=',D15.7,',N =',D15.7,',
     *',/,1X,'NO='
     3,D15.7,',N2=',D15.7,',AR=',D15.7,',T=',F6.1,' &END
30000 FORMAT(//,2X,'CH4 = ',D15.7,2X,'CH3 = ',D15.7,2X,'H ='
     *,D15.7,2X,'
     1OH =',D15.7,2X,'H2O =',D15.7,//,2X,'O =',D15.7,2X,'H2
     * =',D15.7,2X,
     2'O2 =',D15.7,2X,'HCO =',D15.7,2X,'CO =',D15.7,//,2X,'C
     *O2 =',D15.7,
     32X,'N  =',D15.7,2X,'NO =',D15.7,2X,'N2=',D15.7,2X,'AR
     * =',D15.7,//,
     42X,'T =',F6.1,//)
11111 CONTINUE
      STOP
      END
```